Atmos. Chem. Phys. Discuss., https://doi.org/10.5194/acp-2017-606
Manuscript under review for journal Atmos. Chem. Phys.
Discussion started: 13 July 2017

Decadal change of summertime reactive nitrogen species and surface ozone over the Southeast United States

Jingyi Li[1], Jingqiu Mao[2], Arlene M. Fiore[3], Ronald C. Cohen[4,5], John D. Crounse[6], Alex P. Teng[6], Paul O. Wennberg[6,7], Ben H. Lee[8], Felipe D. Lopez-Hilfiker[8], Joel A. Thornton[8], Jeff Peischl[9,10], Ilana B. Pollack[11], Thomas B. Ryerson[9], Patrick Veres[9,10], James M. Roberts[9], J. Andrew Neuman[9,10], John B. Nowak[12,a], Glenn M. Wolfe[13,14], Thomas F. Hanisco[14], Alan Fried[15], Hanwant B. Singh[16], Jack Dibb[17], Fabien Paulot[18,19], Larry W. Horowitz[19]

[1]Jiangsu Key Laboratory of Atmospheric Environment Monitoring and Pollution Control, Collaborative Innovation Center of Atmospheric Environment and Equipment Technology, School of Environmental Science and Engineering, Nanjing University of Information Science and Technology, Nanjing, Jiangsu, 210044, China
[2]Department of Chemistry and Biochemistry & Geophysical Institute, University of Alaska Fairbanks, Fairbanks, Alaska, 99775, USA
[3]Department of Earth and Environmental Sciences & Lamont-Doherty Earth Observatory of Columbia University, Palisades, New York, 10027, USA
[4]Department of Chemistry, University of California, Berkeley, Berkeley, California, 94720, USA
[5]Department of Earth and Planetary Science, University of California, Berkeley, Berkeley, California, 94720, USA
[6]Division of Geological and Planetary Sciences, California Institute of Technology, Pasadena, California, 91125, USA
[7]Division of Engineering and Applied Science, California Institute of Technology, Pasadena, California, 91125, USA
[8]Department of Atmospheric Sciences, University of Washington, Seattle, Washington, 98195, USA
[9]Chemical Sciences Division, NOAA Earth System Research Laboratory, Boulder, Colorado, 80305, USA
[10]Cooperative Institute for Research in Environmental Science, University of Colorado Boulder, Boulder, Colorado, 80309, USA
[11]Department of Atmospheric Science, Colorado State University, Fort Collins, Colorado, 80523, USA
[12]Aerodyne Research, Inc., Billerica, Massachusetts, 01821, USA
[13]Joint Center for Earth System Technology, University of Maryland Baltimore County, Baltimore, Maryland, 21250, USA
[14]Atmospheric Chemistry and Dynamics Lab, NASA Goddard Space Flight Center, Greenbelt, Maryland, 20771, USA
[15]Institute of Arctic & Alpine Research, University of Colorado, Boulder, Colorado, 80309, USA
[16]NASA Ames Research Center, Moffett Field, California, 94035, USA
[17]Department of Earth Sciences and Institute for the Study of Earth, Oceans, and Space, University of New Hampshire, Durham, New Hampshire, 03824, USA
[18]Program in Atmospheric and Oceanic Sciences, Princeton University, Princeton, New Jersey, 08544, USA
[19]Geophysical Fluid Dynamics Laboratory/National Oceanic and Atmospheric Administration, Princeton, New Jersey, 08540, USA
[a]now at: NASA Langley Research Center, Hampton, Virginia, USA

Correspondence to: Jingqiu Mao (jmao2@alaska.edu)

Atmos. Chem. Phys. Discuss., https://doi.org/10.5194/acp-2017-606
Manuscript under review for journal Atmos. Chem. Phys.
Discussion started: 13 July 2017

Abstract

Widespread efforts to abate ozone (O_3) smog have significantly reduced nitrogen oxides (NO_x) emissions over the past two decades in the Southeast U.S. (SEUS), a place heavily influenced by both anthropogenic and biogenic emissions. How reactive nitrogen speciation responds to the reduction in NO_x emissions in this region remains to be elucidated. Here we exploit aircraft measurements from ICARTT (July-August, 2004), SENEX (June-July, 2013), and SEAC^{4}RS (August-September, 2013) and long-term ground measurement networks alongside a global chemistry-climate model to examine decadal changes in summertime reactive nitrogen species and ozone over the Southeast U.S. We find that most reactive nitrogen species, including NO_x, peroxyacetyl nitrate (PAN) and nitric acid (HNO_3) decline proportionally with decreasing NO_x emissions in this region, leading to a similar decline in exported NO_y. This linear response is in part due to the nearly constant summertime supply of biogenic VOC emissions in this region. Our model captures the observed relative change of reactive nitrogen species and surface ozone from 2004 to 2013. Model sensitivity tests indicate that further reductions of NO_x emissions will lead to a continued decline in surface ozone and less frequent extreme ozone events.

1 Introduction

Since the 1990s, the U.S.A. Environmental Protection Agency (U.S. EPA) has targeted emissions of nitrogen oxides (NO_x) to improve air quality by lowering regional photochemical smog (The 1990 Clean Air Amendment). Satellite- and ground-based observations imply significant declines in U.S. NO_x emissions, with a decreasing rate of roughly - 4 % yr^{-1} after 2005 (Krotkov et al., 2016; Russell et al., 2012; Tong et al., 2015; Miyazaki et al., 2017; Lu et al., 2015; Lamsal et al., 2015). This has proven effective at lowering near-surface ozone (O_3) in the past few decades (Cooper et al., 2012; Simon et al., 2015; Hidy and Blanchard, 2015; Stoeckenius et al., 2015; Xing et al., 2015; Yahya et al., 2016). According to U.S. EPA data, the average of the annual 4th highest maximum daily averaged maximum 8-hr (MDA8) ozone over 212 sites has decreased by 33 % from 101 ppb in 1980 to 68 ppb in 2014 across the continental U.S., with more significant reductions in rural areas in summer (Simon et al., 2015; Cooper et al., 2012). Here we combine aircraft and ground-based datasets for both ozone and reactive nitrogen to evaluate a chemistry-climate model used to project future responses to changes in NO_x emissions.

In the troposphere, ozone is produced through photochemical reactions involving NO_x and volatile organic compounds (VOCs) in the presence of sunlight. During photooxidation, a large fraction of NO_x is transformed into its reservoirs, including nitric acid (HNO_3), peroxy nitrates (RO_2NO_2, dominated by peroxyacetyl nitrate (PAN)), and alkyl nitrates ($RONO_2$). These species, together with NO_x, are known as total reactive

nitrogen ($NO_y = NO_x + HNO_3 + HONO + 2 \times N_2O_5$ + total peroxy nitrates (∑PNs) + total alkyl nitrates (∑ANs)). Some of these reservoir species, particularly those with an organic component, tend to be less soluble and longer lived. They may carry reactive nitrogen far from the NO_x source region (Stohl et al., 2002; Parrish et al., 2004; Li et al., 2004) and thereby affect NO_x concentrations and O_3 formation on a regional to global scale (Liang et al., 1998; Horowitz et al., 1998; Perring et al., 2013; Paulot et al., 2016; Hudman et al., 2004).

$RONO_2$ originating from biogenic VOCs (BVOCs) represents a major uncertainty in the NO_y budget, as BVOC emissions account for more than 80 % of global VOC emissions (Millet et al., 2008). To a large extent, this is due to the uncertainties in current understanding of BVOC oxidation chemistry. Biogenic $RONO_2$ species are mainly produced from the oxidation of BVOCs by OH in the presence of NO_x during daytime and by nitrate radical (NO_3) during nighttime. Laboratory and field studies show a wide range of $RONO_2$ yields from their BVOC precursors (Browne et al., 2014; Fry et al., 2014; Lockwood et al., 2010; Paulot et al., 2009; Rindelaub et al., 2015; Rollins et al., 2009; Lee et al., 2014; Xiong et al., 2015; Xiong et al., 2016; Teng et al., 2015). Another uncertainty lies in the fate of $RONO_2$, i.e. recycling $RONO_2$ into NO_x versus converting it to HNO_3 as a NO_x sink have important implications for the NO_y budget and thus O_3 production (Fiore et al., 2005; Horowitz et al., 2007; Ito et al., 2009; Perring et al., 2013; Paulot et al., 2012). In addition, recent field studies have shown that $RONO_2$ is a potential source of secondary organic aerosol (SOA) over the Southeast U.S. (Xu et al., 2015; Lee et al., 2016). The fate of particle-phase $RONO_2$ is unclear, with the possibility for removal by hydrolysis to form HNO_3 (Jacobs et al., 2014; Hu et al., 2011; Darer et al., 2011; Rindelaub et al., 2015; Szmigielski et al., 2010; Sato, 2008; Romer et al., 2016; Wolfe et al., 2015), photochemical aging (Nah et al., 2016; Boyd et al., 2015), and deposition (Nguyen et al., 2015) .

Over the Southeast U.S., photochemistry in summer is strongly influenced by both biogenic and anthropogenic emissions, implying strong sensitivity of O_3 production to changes in anthropogenic NO_x emissions (Simon et al., 2015). Aircraft campaigns during the summers of 2004 and 2013 (i.e. the International Consortium for Atmospheric Research on Transport and Transformation (ICARTT) (Fehsenfeld et al., 2006; Singh et al., 2006), the Southeast Nexus (SENEX) (Warneke et al., 2016), and Studies of Emissions, Atmospheric Composition, Clouds and Climate Coupling by Regional Surveys (SEAC^{4}RS) (Toon et al., 2016)) provide detailed characterization of tropospheric composition in this region separated by nearly a decade. Together with the wet deposition flux of nitrate (NO_3^-) from the National Atmospheric Deposition Program (NADP) and NO_y and O_3 measurements from EPA Air Quality System (AQS) surface network, these aircraft datasets provide insights into changes in O_3 pollution and NO_y speciation over a

decadal period when NO_x emissions were declining rapidly as pollution control programs were implemented.

Here we use a high-resolution global 3D climate-chemistry model, the Geophysical Fluid Dynamics Laboratory (GFDL) AM3 model, with updated isoprene and organic nitrate chemistry to investigate decadal changes of NO_y (and its specific constituents) and surface O_3 during summer between 2004 and 2013 over the Southeast U.S. We first evaluate the model with comprehensive measurements from three aircraft campaigns in the summer of 2004 (ICARTT) and 2013 (SENEX and SEAC^{4}RS). The model estimates of nitrate wet deposition flux are also evaluated against measurements from the NADP; model estimates for NO_y are compared against measurements from EPA AQS to provide an additional constraint on the fate of NO_y species in the model. We then investigate the repartitioning of NO_y species in response to NO_x emission reductions from 2004 to 2013. From there, we examine the model estimate of decadal changes of summertime surface O_3 at 157 monitoring sites over the Southeast U.S. by comparing to the measurements from EPA AQS. Last, we demonstrate the sensitivity of MDA8 O_3 and NO_y speciation to projected NO_x emission decreases over the next decade (to 2022).

2 Methodology

2.1 AM3 Model

We apply a high-resolution (50 x 50 km^2) version of the GFDL AM3 model to study decadal changes of O_3 and organic nitrates over the Southeast U.S. The model configuration is to a large extent similar to that used in a companion paper (Li et al., 2016); and a short summary is provided below. The dynamical core, physical parameterizations, cloud and precipitation processes, and cloud-aerosol interactions mainly follow Donner et al. (2011), except that convective plumes are computed on a vertical grid with finer resolution (Paulot et al., 2016). Dry deposition in the model has been updated to use dry deposition velocities calculated in the GEOS-Chem model (Paulot et al., 2016), to reflect rapid deposition of organic nitrates and oxidized volatile organic compounds (OVOCs) (Nguyen et al., 2015).

Isoprene emissions are computed in the model using the Model of Emissions of Gases and Aerosols from Nature (MEGAN). In July-August of 2004, the computed isoprene emissions over the continental U.S. (25-50° N, 130-70° W) are 8.0 Tg C and appear to be consistent with a previous model estimate of 7.5 Tg C by Mao et al. (2013) in the same region during this period. For 2013, we applied a 20 % reduction of MEGAN for isoprene emissions as described in Li et al. (2016). The resulting isoprene emission is 7.7 Tg C in July-August over this region. Monoterpene emissions follow Naik et al. (2013) and do not vary interannually, with a total of 4.0 Tg C in July and August.

Anthropogenic emissions follow the Representative Concentration Pathway 8.5 (RCP 8.5) projection (Lamarque et al., 2011) for both 2004 and 2013, to compare the model to observations in a consistent fashion. As shown in Table 1, anthropogenic NO_x emissions over the continental U.S. during July-August of 2004 amount to 0.42 Tg N mon^{-1}, consistent with Hudman et al. (2007) but 11 % lower than EPA estimates of 0.47 Tg N mon^{-1} (Granier et al., 2011). For the year of 2013, we apply a 25 % reduction to the anthropogenic NO_x emissions from the RCP 8.5 projection (from base year 2010), to best reproduce the vertical profiles of NO_y species during SENEX as shown below. This adjustment is also consistent with recent estimates of NO_x emissions over the Southeast U.S. (Anderson et al., 2014). The resulting anthropogenic NO_x emissions (0.25 Tg N mon^{-1}) are 14 % lower than NEI11v1 emission inventory estimate (0.29 Tg N mon^{-1}), although both inventories have a similar spatial distribution (Figure S1). Soil NO_x emissions in our model, 3.6 Tg N yr^{-1} globally (Naik et al., 2013), are considerably lower than other model estimates, including 5.5 Tg N yr^{-1} in Yienger and Levy (1995) and 9.0 Tg N yr^{-1} in Hudman et al. (2012). Lightning NO_x, calculated as a function of parameterized convection in the model following Price et al. (1997), is also lower than that of Hudman et al. (2007) by a factor of 8 over the U.S. As a result, the total NO_x emissions over the continental U.S. are 0.98 Tg N for July-August of 2004, and 0.64 Tg N in July-August of 2013 (Table 1). The 40 % reduction of anthropogenic NO_x emissions from 2004 to 2013 over the eastern U.S is consistent with EPA Air Pollutant Emissions Trends Data (https://www.epa.gov/air-emissions-inventories/air-pollutant-emissions-trends-data) and satellite observations (Krotkov et al., 2016; Lu et al., 2015).

2.2 Gas-phase chemistry

We apply the same isoprene mechanism as described by Li et al. (2016). A full list of the reactions can be found in Table S1. This mechanism is based on Mao et al. (2013), but has been significantly revised to incorporate recent laboratory updates on isoprene oxidation by OH and O_3 (Schwantes et al., 2015; Bates et al., 2016; Peeters et al., 2014; St. Clair et al., 2016; Bates et al., 2014; Praske et al., 2015; Müller et al., 2014; Lee et al., 2014; Crounse et al., 2011). One major feature is the suppression of δ-isoprene hydroxyl peroxy radical (δ-$ISOPO_2$) and subsequent reaction pathways in the model, as these channels are considered to be of minor importance under ambient conditions (Peeters et al., 2014; Bates et al., 2014). The fraction of $ISOPO_2$ undergoing isomerization is calculated using bulk isomerization estimates (Crounse et al., 2011). As a result, the first-generation isoprene alkyl nitrate is assumed to be β-hydroxy nitrate (ISOPNB) in the model with a yield of 10 % from the $ISOPO_2$ + NO pathway. This differs from a recent GEOS-Chem study of organic nitrates over the Southeast U.S. that assumed 9 % yield of the first-generation isoprene alkyl nitrate comprised of 90 % ISOPNB and 10 % δ-hydroxy nitrate (ISOPND) (Fisher et al., 2016). The treatment of β- and δ-$ISOPO_2$ will not only affect the speciation of organic nitrates but also the production of O_3 due to

different NO_x recycling efficiency in their secondary products. We also include updated chemistry for methylvinyl ketone (MVK) (Praske et al., 2015), an updated yield of hydroxy hydroperoxides (ISOPOOH) (Bates et al., 2016; St. Clair et al., 2016), fast photolysis of carbonyl organic nitrates (Müller et al., 2014), and an updated ozonolysis rate of ISOPNB (Lee et al., 2014). In addition, we reduce the yield of organic nitrates (MACRN) from methacrolein (MACR) oxidation from 15 % to 3 %, which is estimated from the measured yield of nitrate from MVK oxidation (Praske et al., 2015).

Another major model revision involves the treatment of the nighttime oxidation of isoprene. Instead of following Mao et al. (2013), we revised the nighttime oxidation of isoprene largely based on the Leeds Master Chemical Mechanism v3.2 (MCM v3.2), allowing a more complete description of isoprene oxidation by NO_3. In particular, MCM v3.2 suggests significant production of propanone nitrate (PROPNN) from the photooxidation of the C_5 carbonyl nitrate, consistent with recent laboratory experiments (Schwantes et al., 2015). We also updated the products of the reaction of nitrooxy alkylperoxy radical (INO_2), the peroxy radical from isoprene oxidation by NO_3, with HO_2 to reflect a lower molar yield (0.77) of C_5 nitrooxy hydroperoxide (INPN) (Schwantes et al., 2015). The differences between MCM v3.2 and the most updated version, MCM v3.3.1, in isoprene nighttime chemistry appears to be small (Jenkin et al., 2015). We therefore use MCM v3.2 as the reference in this work.

We include a highly simplified chemistry for the oxidation of monoterpenes in this work, mainly to quantify their contribution to organic nitrates. Monoterpenes are lumped into one chemical species ($C_{10}H_{16}$) in our model. The organic nitrate yield is set to 26 % from OH-initiated oxidation (Rindelaub et al., 2015) and to 10 % from NO_3-initiated oxidation (Browne et al., 2014). Details of the monoterpene chemistry can be found in Table S2.

2.3 Heterogeneous loss of organic nitrates

Field and laboratory studies have indicated a potential contribution to aerosol formation of organic nitrates from BVOC oxidation (Ayres et al., 2015; Fry et al., 2014; Nah et al., 2016; Rollins et al., 2009; Rindelaub et al., 2015; Boyd et al., 2015; Lee et al., 2016; Ng et al., 2008; Fry et al., 2009; Xu et al., 2015; Lee et al., 2014; Bean and Hildebrandt Ruiz, 2016; Spittler et al., 2006). Aerosol yield depends on both the VOC precursor and the oxidant. For example, Δ-3-carene oxidation by NO_3 can produce a 38-65 % yield of organic aerosols in a smog chamber (Fry et al., 2014), which is much higher than the 1-24 % yield from NO_3-initiated isoprene oxidation (Ng et al., 2008; Rollins et al., 2009; Ayres et al., 2015). Recent chamber studies indicate a very low aerosol yield from α-pinene oxidation by NO_3 (Nah et al., 2016; Fry et al., 2014),the aerosol yield increases to ~ 18 % when α-pinene is oxidized by OH (Rollins et al., 2010; Rindelaub et al., 2015). It should be noted that these results from laboratory experiments might not be

representative to atmospheric conditions in terms of the RO_2 reaction partner or RO_2 lifetime.

In the condensed phase, organic nitrates can undergo hydrolysis reactions to produce HNO_3 (Darer et al., 2011; Hu et al., 2011; Rindelaub et al., 2015; Boyd et al., 2015; Szmigielski et al., 2010; Sato, 2008; Jacobs et al., 2014; Bean and Hildebrandt Ruiz, 2016). However, the hydrolysis rate varies greatly with the structure of nitrate, and for most species remains highly uncertain, though certain trends have been elucidated, e.g. tertiary nitrates favor hydrolysis while primary and secondary nitrates are more stable (Bean and Hildebrandt Ruiz, 2016; Darer et al., 2011; Hu et al., 2011; Boyd et al., 2015). Here we assume a first-order irreversible reactive uptake for the heterogeneous loss of organic nitrates onto aerosols (R1), followed by its hydrolysis reaction returning HNO_3 and alcohols (R2) (Fisher et al., 2016):

$$RONO_2(g) \xrightarrow{k_1} AONJ(aq) \tag{R1}$$

$$AONJ(aq) + H_2O \xrightarrow{k_2} ROH + HNO_3(g) \tag{R2}$$

where $RONO_2$, AONJ and ROH represent gas- and particle-phase organic nitrates and alcohols respectively. For the daytime isoprene organic nitrates (mainly from the $ISOPO_2$ + NO pathway), we only consider heterogeneous loss of ISOPNB to aerosols, since this has been detected in field and laboratory studies (Jacobs et al., 2014). Lee et al. (2014) hypothesized a significant amount of C_5 dinitrate (DHDN, with a molar yield of 21 % via the ISOPNB peroxy radical + NO pathway) produced from OH oxidation of ISOPNB. Since DHDN is highly functionalized and might partition to the condensed phase forming SOA, we test the impact of this process on the estimate of NO_y speciation and O_3 concentration in a sensitivity study (AM3h, Figure S2). Aerosol formation from nighttime isoprene organic nitrates (from isoprene oxidation by NO_3) are neglected due to the low mass yields. Information about hydrolysis of daytime monoterpene nitrates (from OH oxidation of monoterpenes) is quite sparse. Two chamber studies to date have examined the hydrolysis of nitrates from α-pinene oxidation by OH (Rindelaub et al., 2015; Bean and Hildebrandt Ruiz, 2016). They found that the hydrolysis rate is dependent on relative humidity (RH) and aerosol acidity. We also examine the hydrolysis of daytime monoterpene nitrates (TERPN1) in the above sensitivity study (AM3h, Figure S2). We do not consider heterogeneous loss of nighttime monoterpene nitrates in this work due to inadequate information.

We allow heterogeneous loss of organic nitrates to sulfate, black carbon, primary organic carbon, sea salt, mineral dust and SOA following Li et al. (2016). The first-order rate constant k_1 is determined using an effective uptake coefficient 0.005 for isoprene nitrates (ISOPNB in all hydrolysis cases and DHDN in AM3h, equivalent to 1.8-h lifetime in the atmosphere) and 0.01 for daytime monoterpene nitrates (TERPN1, in AM3h) following

Fisher et al. (2016), which are consistent with other estimates (Wolfe et al., 2015; Marais et al., 2016). Due to the large uncertainties of lifetimes against hydrolysis, we assume a 3-h bulk lifetime for the three particle-phase nitrates following Pye et al. (2015), consistent with recent estimate of organic nitrate aerosol lifetime at a ground monitoring site in Centreville, Alabama (CTL) (Lee et al., 2016). We also conduct another sensitivity test (AM3 w/o hydro in Figure 1 and Figure 2) without accounting for the heterogeneous loss of organic nitrates.

3 Observational datasets

We use measurements from a series of field campaigns (2004 ICARTT, 2013 SENEX, and 2013 SEAC^{4}RS) to evaluate the performance of the model in estimating O_3, NO_x, HNO_3, PAN, ∑ANs and NO_y over the Southeast U.S. during summer.

The ICARTT aircraft campaign provided a detailed characterization of tropospheric chemistry over the eastern U.S. in the summer of 2004 (July 1-August 15, 2004). Two aircraft, the NASA DC-8 and the NOAA WP-3D, were deployed to collect measurements of ozone, NO_y species, isoprene and its oxidation products. Here we focus on data including O_3, NO_x, HCHO (Tunable Diode Laser (TDL) absorption spectrometry), HNO_3 (mist chamber/IC by University of New Hampshire and Chemical Ionization Mass Spectrometer (CIMS) by California Institute of Technology), PAN and ∑ANs (including gas and aerosol $RONO_2$) from 11 science flights on the NASA DC-8 aircraft over the Southeast U.S. Details of the instrument operation and accuracy are summarized in Singh et al. (2006) and references therein.

SENEX was a NOAA aircraft campaign aimed to investigate the interaction between biogenic and anthropogenic emissions and the formation of secondary pollutants over the Southeast U.S. in summer 2013 (May 27-July 10, 2013). The NOAA WP-3D aircraft was launched to collect measurements of a variety of chemical compounds during 18 scientific flights. Here we focus on data, including O_3, NO_x, HNO_3, PAN and NO_y from 15 daytime flights only. We also used measurements of ISOPN, methylvinylketone nitrates (MVKN) and methacrolein nitrates (MACRN) taken by University of Washington from 10 daytime flights during June 3-July 3 of the campaign. Details of the instrument operation and accuracy are summarized in Warneke et al. (2016) and references therein.

Because ∑ANs and several speciated $RONO_2$ were not measured on the NOAA WP-3D aircrafts during SENEX, we include another aircraft campaign for model evaluation despite that this campaign has a major coverage in September of 2013. SEAC^{4}RS was a NASA aircraft campaign with the field mission based in Houston, Texas during August-September 2013, designed to examine vertical transport of atmospheric pollutants from the surface to the stratosphere. It provides comprehensive measurements of atmospheric

composition in the lower troposphere over North America. Here we use observations of O_3, NO_2, HCHO (laser-induced fluorescence, LIF), ∑ANs (including gas and aerosol $RONO_2$) and speciated $RONO_2$ from 20 NASA DC-8 science flights to evaluate the correlations of ∑ANs and major $RONO_2$ originating from isoprene oxidation during daytime with O_x (= O_3 + NO_2) and with HCHO, respectively, as additional constraints to the model. Details of the instrument operation and accuracy are summarized in Toon et al. (2016) and references therein. We mainly focus on $RONO_2$ and related species from SEAC^{4}RS in this work.

Besides these aircraft campaigns, we also use surface observations for model evaluation, including nitrate (NO_3^-) wet deposition flux and concentration from the National Trend Network (NTN) of NADP (accessible at http://nadp.sws.uiuc.edu/data/) and surface O_3 from EPA AQS (accessible at https://aqs.epa.gov/aqsweb/documents/data_mart_welcome.html). NTN provides the monthly NO_3^- concentration and precipitation so that the monthly mean concentration of NO_3^- and wet deposition flux could be derived for model evaluation. The AQS database provides measurements of important ambient air pollutants (O_3, NO_x, SO_2, $PM_{2.5}$ species, etc.) collected at monitoring sites across the continental U.S. We focus on NO_3^- wet deposition fluxes at 53 sites (Figure 3) and MDA8 O_3 at 157 sites (Figure S3) located in the Southeast U.S. during July-August of 2004 and 2013.

4 Model evaluation of ozone and reactive nitrogen species

We evaluate our model against observations from aircraft campaigns in 2004 and 2013. For each of the three field campaigns, all measurements are averaged to a 1-min time resolution. Data from biomass burning (CH_3CN ≥ 225 ppt or HCN ≥ 500 ppt), urban plumes (NO_2 ≥ 4 ppb or NO_x/NO_y ≥ 0.4 (if NO_y is available)), and stratospheric air (O_3/CO >1.25 mol mol^{-1}) are excluded (Hudman et al., 2007) in all the analyses. We focus on the Southeast U.S. region, using only data within the domain of 25-40° N latitude and 100-75° W longitude for our analyses. A map of all the flight tracks of each campaign is shown in Figure S4. All model results for comparison with observations use model output sampled along the flight track with 1-min time resolution.

4.1 Mean vertical profiles of O_3 and reactive nitrogen species

Figure 1 shows the observed and modeled mean vertical profiles of O_3, NO_x, HNO_3, PAN, ∑ANs and NO_y during ICARTT and SENEX. We use ∑ANs measurements from SEAC^{4}RS to evaluate model performance during summer 2013, due to the lack of ∑ANs measurements from SENEX. Our model results include both gas and aerosol $RONO_2$ in ∑ANs, although aerosol $RONO_2$ accounts for 7~11% of ∑ANs in the boundary layer (BL, < 1.5 km).

Mean observed O_3 in the surface layer decreased from 50 ppb during ICARTT to 35 ppb during SENEX, consistent with the decline in surface MDA8 ozone at AQS monitoring sites during July-August from 2004 to 2013 over the Southeast U.S. as shown below. Differences in meteorology may account for some of this decline as this region was cool and wet in Summer 2013 (Hidy et al., 2014), conditions that suppress ozone formation. We show below that this impact is relatively small compared to that from NO_x emission reductions in this region. Our model can reproduce the vertical gradient of O_3 as well as the relative change from 2004 to 2013, but the model has a positive bias of upto 6 ppb and 12 ppb in the boundary layer during ICARTT and SENEX respectively. This overestimate of O_3 appears to be higher than that reported (3-5 ppb) by Mao et al. (2013) for their simulation of the ICARTT dataset, likely due to faster photolysis of carbonyl nitrates that increases the NO_x recycling efficiency from isoprene oxidation. A recent study using the GEOS-Chem model (Travis et al., 2016) shows that this regional bias can be reduced (though not eliminated) with a 53 % reduction of anthropogenic NO_x emissions from the 2011 EPA national emission inventory (NEI11v1). Despite some evidence of overestimated NO_x emissions in NEI11v1 (Souri et al., 2016; Ahmadov et al., 2015), we find that such a reduction of NO_x emissions would lead to a significant underestimate of the simulated vertical profiles of reactive nitrogen oxides in our model, as we show below. Therefore, we conclude that the bias in the vertical profile of O_3 in our model, even though the cause is not entirely understood so far, may not be solely due to biases in NO_x emissions.

We further examine mean vertical profiles of NO_x and its reservoirs in 2004 and 2013. In the boundary layer along the flight tracks (Figure 1), HNO_3 is the most abundant reactive nitrogen compound, accounting for 40-46 % of NO_y, followed by NO_x (18-23 %), PAN (21 %), and ∑ANs (11-21 %). Between 2004 and 2013, mean observed NO_y in the boundary layer decreased by 20 %, from 2.0 ppb to 1.6 ppb, a weaker change than the 35 % reduction of total NO_x emissions (Table 1). This is likely due to the different sampling regions (Figure S4) from the two campaigns. We show later that regionally-averaged NO_y indicates a 34 % reduction over the Southeast U.S. from 2004 to 2013, more consistent with the emission reductions (- 35 %). The responses of major reactive nitrogen compounds are mostly proportional to the change in NO_x emissions, with the notable exception of ∑ANs. We find significant decreases in NO_x (- 35 %) and HNO_3 (- 29 %) as well as a slight decrease in PAN (- 13 %) from observations. The relative trends of HNO_3 and PAN are opposite to those found in the Los Angeles (LA) basin, where PAN decreased much faster than HNO_3 (Pollack et al., 2013). This difference results mainly from the rapid decrease of anthropogenic VOC emissions in the LA basin that also serves as major precursors of PAN. In contrast, BVOC emissions show a constant supply (within 5 % differences over the two summers) over the Southeast U.S. ∑ANs shows a different trend from the above compounds, increasing from 0.23 ppb to 0.27 ppb (+ 17 %) near the surface (Figure 1). As we show below, these changes (except for ∑ANs)

are mostly consistent with model estimates on a regional average, despite possible representativeness errors from different sampling areas during the three aircraft campaigns (Figure S4).

The model can well reproduce all the NO_y species in the boundary layer but tends to underestimate them in the free troposphere. This is likely due to insufficient production of NO_x from lightning in the free troposphere in our model, which is 0.048 Tg N in total over North America during July-August of 2004, lower by almost a factor of 5 compared to the value (0.27 Tg N from July 1-August 15, 2004) reported by Hudman et al. (2007). Underestimate of NO_x in the free troposphere might also be due to rapid conversion of NO_x to HNO_3 (Henderson et al., 2011) in the model. However, we did not adjust the model due to the high uncertainty in the estimate of lightning NO_x. We find that if we reduce anthropogenic NO_x emission in our model by another 40 %, from 0.25 Tg N mon^{-1} to 0.15 Tg N mon^{-1} as suggested by Travis et al. (2016), simulated NO_y, HNO_3 and PAN decrease by 30 %, 33 % and 30 % respectively, leading to a noticeable underestimate for these nitrogen reservoirs.

Hydrolysis of organic nitrates affects $RONO_2$ significantly in the boundary layer. By introducing hydrolysis of ISOPNB, we find that model bias of ∑ANs in the boundary layer is reduced from + 20 % to + 2 % during ICARTT (Figure 1). However, the bias is increased in magnitude from – 9 % to – 24 % during SEAC^{4}RS. This low bias can be partially due to neglecting small alkyl nitrates, which could contribute 20-30 ppt to ∑ANs (Fisher et al., 2016). Hydrolysis of ISOPNB also impacts its product HNO_3. Although the change in HNO_3 is not as evident as that of $RONO_2$, model bias is slightly increased during ICARTT but improved during SENEX. We find that the impact of hydrolysis of ISOPNB on boundary layer O_3 appears to be small. This is mainly because without hydrolysis, the dominant loss of ISOPNB is oxidation by OH, which then leads to the formation of secondary organic nitrates including MVKN, MACRN and a C5 dihydroxy dinitrate (DHDN). The majority of these organic nitrates (MVKN and DHDN) return NO_x slowly due to long lifetimes, resulting in a similar effect on ozone production as hydrolysis of ISOPNB. Besides the good agreement of ∑ANs, our model shows good agreement with speciated $RONO_2$ measured during SENEX and SEAC^{4}RS, including ISOPN and the sum of MVKN and MACRN (Figure 2). We find that the large discrepancy between ∑ANs and speciated alkyl nitrates (Figure S5) can be explained by a combination of terpene nitrates and the C5 dihydroxy dinitrate and nighttime NO_3 oxidation products from isoprene, accounting for 20-24 %, 14-17 % and 23-29 % of ∑ANs in the boundary layer. Contribution of the three types of alkyl nitrates also show different vertical trend. For clarification, all model results discussed below are from AM3 with hydrolysis of ISOPNB.

4.2 NO_3^- wet deposition flux and concentration

Figure 3 shows a comparison of NO_3^- wet deposition flux between observations and model results during the summers of 2004 and 2013. The observed NO_3^- wet deposition flux is calculated by multiplying the measured NO_3^- concentration and precipitation at each monitoring site as $F_{o,i}=C_{o,i}P_{o,i}$, where $F_{o,i}$ is the monthly-mean NO_3^- wet deposition flux, $C_{o,i}$ and $P_{o,i}$ are the monthly-mean observed NO_3^- concentration precipitation at monitoring site i. The modeled NO_3^- wet deposition flux includes HNO_3 and all the alkyl nitrates. Observations indicate a 24 % reduction of NO_3^- wet deposition flux in summer from 2004 to 2013 over the Southeast U.S., likely due to NO_x emission reductions. This reduction in monthly averaged NO_3^- wet deposition flux is well captured by our model (-29 %), despite model has a low bias of 40 % in both years.

Since errors in modeled precipitation could strongly affect the modeled NO_3^- wet deposition flux (Appel et al., 2011; Grimm and Lynch, 2005; Metcalfe et al., 2005; Paulot et al., 2014; Tost et al., 2007), we also evaluate the modeled NO_3^- concentration ($C_{p,i}$), which is calculated by using the modeled NO_3^- wet deposition flux ($F_{p,i}$) and observed precipitation ($P_{o,i}$; $C_{p,i}= F_{p,i}/P_{o,i}$), as a separate constraint. The model shows a similar declining trend from the observations with a bias of - 18 % and – 40 % on NO_3^- concentration for 2004 and 2013 respectively. Our results are consistent with the base case of Paulot et al. (2016), which showed that convective removal is likely insufficient in AM3, leading to underestimates of both NO_3^- wet deposition flux and concentrations. Our results are somewhat different from a recent GEOS-Chem study (Travis et al., 2016). They found that reducing anthropogenic NO_x emissions from NEI11v1 by 60 % can significantly improve the overestimate of 71 % on NO_3^- wet deposition flux in their model during August-September 2013. A further reduction of anthropogenic NO_x emission in our model (to 0.15 Tg N mon^{-1}), as suggested in the previous study, would lead to an even greater negative bias compared to observations.

4.3 $RONO_2$ Chemistry

$RONO_2$ can serve as either a temporary NO_x reservoir by releasing NO_2 via photooxidation or a permanent NO_x sink via hydrolysis to produce HNO_3. The modeled fate of $RONO_2$ affects simulated O_3. Therefore, it is necessary to evaluate the $RONO_2$ chemistry and to understand its speciation.

The major pathway for the production of daytime $RONO_2$ is the reaction of NO with RO_2 originating from VOC oxidation by OH:

$$RH + OH + O_2 \rightarrow RO_2 + H_2O \quad \text{(R3)}$$

$$NO + RO_2 \rightarrow (1 - \alpha)\ NO_2 + \alpha\ RONO_2 + HCHO + \text{products} \quad \text{(R4)}$$

where α is the branching ratio for alkyl nitrate formation. NO_2 subsequently further undergoes photolysis to produce O_3:

$$NO_2 + h\nu \xrightarrow{O_2} O_3 + NO \qquad \text{(R5)}$$

For isoprene, α is 9 ± 4 % (for ISOPN) according to a recent study (Xiong et al., 2015). For monoterpenes, specifically α-pinene, α ranges from 1 % to 26 % (Rindelaub et al., 2015; Nozière et al., 1999; Aschmann et al., 2002). Here, we use 10 % for isoprene and 26 % for monoterpenes (Table S2), and take α as an average of $RONO_2$ from all the precursors. As $RONO_2$ and O_3 are both produced from (R4), a correlation between them is expected. We show that the model can roughly reproduce the correlation of O_x vs. ∑ANs during both ICARTT and SEAC^{4}RS (Figure 4), although the slope has a positive bias of about 21 % and 33 % respectively, largely due to an overestimate of O_3 in the model. In particular, we find that the model shows better agreement with the observed correlation of O_x vs. daytime isoprene nitrates (the sum of ISOPN, MVKN and MACRN) than O_x vs. ∑ANs during SEAC^{4}RS. This is expected since these three $RONO_2$ species are directly coproduced with O_3 from (R4), but only account for a small fraction of ∑ANs (Figure S5). The good agreement between observed and modeled O_x vs. daytime $RONO_2$ provides additional support for our treatment of the yields and fate of these daytime isoprene nitrates.

Another metric to evaluate $RONO_2$ chemistry is the correlation between ∑ANs and HCHO, as the latter is a coproduct from (R4). Since HCHO can be produced from other pathways of isoprene hydroxyl peroxy radicals ($ISOPO_2$) besides (R4) (such as isomerization of $ISOPO_2$ and $ISOPO_2$ + HO_2), changes in the slope of ∑ANs vs. HCHO may help to quantify decadal changes in isoprene oxidation pathways. We show in Figure 4 that the model can roughly capture the observed ∑ANs-HCHO slope, with an underestimate by 25 % and 13 % during ICARTT and SEAC^{4}RS, respectively. The underestimate is in part due to small alkyl nitrates that are neglected in the model, as mentioned above. During ICARTT, the slope estimated by AM3 is 0.12, similar to the value (0.15) from a previous GEOS-Chem study using a different isoprene oxidation mechanism that assumed a higher α (of 11.7 % from both ISOPNB and ISOPND vs. 10 % of ISOPNB and zero ISOPND in AM3) and a lower yield of HCHO (66 % vs. 90 % in AM3) (Mao et al., 2013). The reason for such similarity between the two models might be two-fold: (a) the additional contribution of monoterpene nitrates to ∑ANs in AM3 compensates for the decrease in α from isoprene nitrates compared to GEOS-Chem and (b) the coarse grid resolution of that GEOS-Chem simulation (2° x 2.5°) may lead to a higher estimate of HCHO compared to the result from a finer grid resolution (Yu et al., 2016).

We find in Figure 4 that the observed slope of ∑ANs-HCHO shows very little change from 2004 to 2013. This is in part due to substantial HCHO production from isoprene oxidation under low NO_x conditions (Li et al., 2016), and in part due to the buffering of ∑ANs in response to decreasing NO_x, as shown below. Our model is able to reproduce such behavior. We also find in our model that the branching ratios for the reactions of $ISOPO_2$ change marginally from 2004 to 2013 over the Southeast U.S. (Figure S6). The fraction of $ISOPO_2$ + NO has decreased from 81 % in 2004 to 66 % in 2013. The fraction of $ISOPO_2$ + HO_2 has increased from 15 % to 28 %, and the fraction of $ISOPO_2$ isomerization has increased from 4 % to 6 %. Our result is slightly different from the results of GEOS-Chem, which found a lower contribution from the NO pathway (54 %) and higher from isomerization (15 %) during August-September of 2013 (Travis et al., 2016).

We also compare the correlation between major daytime isoprene nitrates and HCHO during 2013, which provides a constraint on the yield of these nitrates. Our model shows a slight overestimate on the slope (Figure 4 (b)), consistent with comparison of mean vertical profiles shown in Figure 2. The estimated slope (5 %) in this study is different from that (2.5 %) of a recent GEOS-Chem simulation by Fisher et al. (2016). This is partially due to the different treatment of β- and δ-$ISOPO_2$ between GEOS-Chem and AM3. Another factor is that MVKN and MACRN are not allowed to hydrolyze in AM3, leading to a higher burden of these two nitrates.

Figure 5 shows the mean vertical profiles of modeled monoterpene nitrates (MNs) and isoprene nitrates (INs) during ICARTT and SEAC^{4}RS. INs are the most abundant $RONO_2$, accounting for 76-80 % below 3 km over the Southeast U.S., consistent with the large isoprene emissions in this region in summer (Palmer et al., 2003). In the measurements, ISOPN + MVKN + MACRN only contribute one third of the total INs (Figure S5). We show below that the discrepancy of ∑ANs and speciated $RONO_2$ can be explained by other daytime and nighttime INs in the model. More than 60 % of modeled INs originate from isoprene oxidation during daytime. The first-generation nitrate ISOPN contributes slightly more (31 %) than the second-generation nitrates MVKN + MACRN (28 %) to the total daytime INs during ICARTT. This is different from Mao et al. (2013) who showed a higher contribution of MVKN + MACRN than the first-generation INs, due to the different treatment of β- and δ-$ISOPO_2$. We see more ISOPN (32 %) than MVKN + MACRN (26 %) from the daytime INs during SEAC^{4}RS, consistent with Fisher et al. (2016). A large uncertainty in our model is attributed to DHDN, which contributes 32 % to the daytime INs. Fisher et al. (2016) showed less DHDN during SEAC^{4}RS since it was removed rapidly by hydrolysis (1-h lifetime) in their model. Our sensitivity test (AM3h, Figure S2) indicates that AM3 would significantly underestimate ∑ANs if we assume a similar heterogeneous loss as ISOPN. In fact, DHDN was hypothesized originally in Lee et al. (2014) for the imbalance of nitrogen in their lab

experiments, and may serve as a proxy for a large number of unidentified daytime INs. It remains unclear what the dominant loss of DHDN is. Daytime nitrates from monoterpene oxidation are another important source of ∑ANs in this region, accounting for 17-20 % (24-26 ppt) of the total. Fisher et al. (2016) estimate a smaller burden of MNs, of about 10-20 ppt due to a lower molar yield (18 % vs. 26 % in AM3) and faster hydrolysis of MNs in their model.

Nighttime chemistry contributes about 30-36 % of ∑ANs, which is dominated by isoprene oxidation as well (Figure 5). 33-41 % of the INs are produced during night, similar to the value (44 %) reported by Mao et al. (2013) but with different speciation, due to the different treatment of chemistry. PROPNN contributes about 29-38 % of the total INs. PROPNN in this work is mainly produced from the oxidation of C5 carbonyl nitrate (ISN1) and C5 nitrooxy hydroperoxide (INPN) (dominantly by photolysis) that are generated from isoprene oxidation by NO_3 during the nighttime. This is different from Fisher et al. (2016), who showed that PROPNN is partially from the δ-$ISOPO_2$ + NO pathway and partially from the oxidation of ISN1 and INPN. In our model, we see prompt production of PROPNN after sunrise in the boundary layer (Figure S7), consistent with observations at the Southern Oxidants and Aerosols Study (SOAS) ground site CTL (Schwantes et al., 2015). Our model overestimates the mean vertical profile of PROPNN by a factor of 3 (not shown). As our model may largely underrepresent the chemical complexity of nighttime isoprene oxidation as shown by Schwantes et al. (2015), we consider PROPNN as a proxy for other unspecified isoprene nighttime nitrates. As a result, PROPNN contributes a significant fraction of ∑ANs in the model.

5 Decadal Change of PBL NO_y species and surface ozone over SEUS

5.1 NO_y species

We examine the simulated decadal change of NO_y species in the boundary layer over the Southeast U.S. Figure 6 shows the mean modeled boundary layer concentrations of NO_x, HNO_3, ∑PNs, ∑ANs and NO_y in the summer of 2004 and 2013 as well as a scenario with a further 40 % reduction from 2013 anthropogenic NO_x emissions to simulate possible future emission reductions. In summer 2004, modeled NO_y is mainly comprised of HNO_3 (45 %), NO_x (31 %), ∑PNs (14 %) and ∑ANs (9 %). In response to imposing a 40% reduction in anthropogenic NO_x emissions (35 % reduction in total NO_x emissions, Table 1) from 2004 to 2013, NO_y declined by 34 %. This modeled response is consistent with long-term NO_y measurements from AQS dataset, which shows on average a 42 % decrease from 2004 to 2013 over the Southeast U.S. Most NO_y species are reduced proportionally, with decreases of 38 % for HNO_3, 32 % for NO_x and 34% for ∑PNs. The different change in ∑PNs and PAN (the majority of ∑PNs) in Figure 1 might be due to

the difference in sampling regions. The only exception is ∑ANs, with a smaller decline of 19 %. It should be noted that the change of ∑ANs discussed here is different from the surface concentrations discussed in Section 4.1.

We conducted a sensitivity test with an additional 40 % reduction of anthropogenic NO_x emissions from 2013 (Table 2). We find that NO_y decreases by 29 %, with a proportional decrease in HNO_3, NO_x, and ∑PNs. Again, we find that ∑ANs decrease at a slower rate, becoming a larger fraction of total NO_y. The buffering of ∑ANs is consistent with previous studies (Browne and Cohen, 2012; Fisher et al., 2016), mainly due to decreasing NO_x leading to lower OH (Figure S8) and thus a prolonged lifetime of NO_x and ∑ANs (Browne and Cohen, 2012). As shown in Figure S8, averaged noontime OH decreases by 11 % from 2004 to 2013 and by 29 % after we impose an additional 40 % NO_x emission reduction from 2013 levels.

The historical NO_x emission reduction also affects reactive nitrogen export out of the boundary layer. Here we define exported nitrogen as the difference of the sources (chemical production and emissions) and sinks (chemical loss, wet and dry deposition). As shown in Table 2, total summertime NO_y export from the Southeast U.S. boundary layer decreases proportionally, from 24.1 Gg N in 2004 to 16.6 Gg N in 2013. The NO_y export efficiency, calculated as net exported nitrogen divided by total NO_x emissions, remains roughly the same (12 %) for 2004 and 2013, consistent with previous studies (Fang et al., 2010; Li et al., 2004; Parrish et al., 2004; Mao et al., 2013; Sanderson et al., 2008; Hudman et al., 2007). Among all exported species, NO_x contributes most of net export from the PBL (6 % of total NO_x emissions), followed by PAN (4 %) and ∑ANs (2 %). We emphasize in Table 2 that a major fraction of NO_x is exported through the top of the boundary layer (convection). From a budget calculation throughout the tropospheric column over the same region, we find that despite being the same NO_y export efficiency (12 %), HNO_3 becomes the major exporter, accounting for half of NO_y export efficiency from the total column (6 %). The contributions from PAN and ∑ANs are roughly the same as their export from the boundary layer (4 % and 2 %). This suggests that surface NO_x ventilated through the boundary layer, converted to HNO_3 in the free troposphere and exported as HNO_3 is likely the major NO_y export mechanism over the Southeast U.S. in our model, which is in agreement with previous observations (Parrish et al., 2004; Neuman et al., 2006). PAN and ∑ANs together account for another half of NO_y export efficiency. As PAN and ∑ANs are of biogenic origin and longer lived than HNO_3, they may play a key role in influencing reactive nitrogen and ozone in downwind regions (Moxim et al., 1996; Fischer et al., 2014).

5.2 Surface ozone

Understanding oxidation chemistry of NO_x and VOCs is essential to improve surface ozone air quality by implementing effective control strategies. Since the mid-1990s, NO_x emission controls have led to significant improvement on ozone air quality over the eastern U.S. (Simon et al., 2015; Cooper et al., 2012). As NO_x emissions continue to decrease, ozone production efficiency (OPE) may increase due to the lower NO_x removal rate by OH and to some extent may compensate the ozone reduction (Sillman, 2000). Meanwhile, surface ozone production may be further complicated by the increasing importance of $ISOPO_2$ isomerization (Peeters et al., 2014). Here we first evaluate our model against surface ozone observations in 2004 and 2013, and then project the future response of surface ozone to even lower NO_x emissions to examine the efficacy of near-term NO_x emission controls at lowering near-surface ozone levels.

We first examine the modeled surface ozone against observations at 157 EPA AQS monitoring sites over the Southeast U.S. in July-August of 2004 and 2013 (Figure S9). In general, AM3 overestimates surface MDA8 ozone in both years by about 16 ppb on average. This positive bias of summertime surface O_3 has been a common issue to a number of modeling studies of this region (Fiore et al., 2009; Canty et al., 2015; Brown-Steiner et al., 2015; Strode et al., 2015; Travis et al., 2016). This might be partially attributed to overestimated anthropogenic NO_x emissions from non-power plant sectors, excessive vertical mixing in the boundary layer (Travis et al., 2016) or underestimates of O_3 dry deposition (Hardacre et al., 2015; Val Martin et al., 2014). Further studies are warranted to investigate the cause of this bias in AM3.

Surface O_3 concentrations over the Southeast U.S. decline substantially from 2004 to 2013 in response to the large NO_x emission reduction (Simon et al., 2015). MDA8 ozone averaged across all the monitoring sites is observed to decrease by 11 ppb (23 % of observed mean MDA8 ozone in July-August of 2004) resulting from approximately 40 % reductions of anthropogenic NO_x emissions (35 % reduction in total NO_x emissions) across the continental U.S. This strong sensitivity of surface ozone to NO_x emission reflects the linear relationship between ozone production rate and NO_x concentrations when NO_x is low (Trainer et al., 2000). In contrast, the sensitivity of surface ozone to NO_x emissions appears to be weaker in the 1980s. Jacob et al. (1993) found that summertime afternoon ozone over the eastern U.S. is only reduced by 15 % with a 50 % reduction of anthropogenic NO_x emissions from 1985 levels, suggesting a lower OPE when NO_x concentrations were high. We attribute this transition from a low OPE in the 1980s to high OPE in 2000s to the extended lifetime of NO_x resulting from NO_x emission reductions. Our model is able to capture this strong NO_x-O_3 sensitivity, with the mean MDA8 ozone reduced by 10 ppb from 2004 to 2013. We find that a further 40 % reduction of anthropogenic NO_x emissions with identical meteorological conditions and non-anthropogenic emissions in 2013 could lead to an additional 9 ppb decrease, a similar magnitude to the change from 2004 to 2013. Meanwhile, any increase in OPE

over the past decade appears to be small and to have little impact on net ozone production, leading to a continued high sensitivity of surface ozone to NO_x emission reductions in the near future.

We further investigate the impact of temperature and moisture on surface O_3 from 2004 to 2013. While several studies suggest that surface O_3 increases with ambient temperature (Jacob and Winner, 2009; Bloomer et al., 2010; Wu et al., 2008; Steiner et al., 2010), Cooper et al. (2012) showed that this temperature related impact is weak during the period of 1990-2010 across the USA. Recent studies suggest that relative humidity (RH) or vapor pressure deficit (VPD) may play an important role in ozone variability through soil-atmosphere or biosphere-atmosphere coupling (Kavassalis and Murphy, 2017; Camalier et al., 2007; Tawfik and Steiner, 2013). Our model shows marginal differences in RH and temperature over the Southeast U.S. between the summers of 2004 and 2013, consistent with climatology data (Hidy et al., 2014). Using the same model but with the standard AM3 chemical mechanism, Lin et al. (2017) found that meteorology changes would have caused surface ozone over the eastern U.S. to increase in the absence of emission controls from 1999 to 2014. Therefore, we conclude that the impact of climate variability and change on O_3 is relatively small compared to NO_x emission reductions over the Southeast U.S., consistent with previous studies (Lam et al., 2011; Hidy et al., 2014; Lin et al., 2017; Rieder et al., 2015)

Decreasing NO_x emission also reduces the frequency of extreme O_3 pollution events. Figure 7 shows the probability density function of observed and modeled MDA8 ozone at each monitoring site during July-August of 2004 and 2013, and the probability density function of modeled MDA8 ozone under a future scenario with another 40 % reduction in anthropogenic NO_x emissions compared to 2013. We show that the lowest O_3, about 20 ppb in current model simulations, remains invariant with NO_x emission changes over the Southeast U.S., consistent with observations (Figure 7 (a)). Meanwhile, the high tail of MDA8 ozone events has shifted from more than 100 ppb in 2004 to about 85 ppb after the 40% reduction of anthropogenic NO_x emissions from 2013. A similar shift is found in observations. The narrowing of the range of O_3 with decreasing NO_x is consistent with the observed trends reported by Simon et al. (2015). We also find that further reductions of NO_x emissions will reduce both median O_3 values and the high tail, suggesting that fewer extreme ozone events will occur under continued NO_x emission controls in the future.

6 Conclusions and Discussions

Near-surface ozone production over the Southeast U.S. is heavily influenced by both anthropogenic and biogenic emissions. We investigate the response of NO_y speciation to such NO_x reduction to the significant NO_x emission controls (about 40 % reductions) in this region over the past decade, in light of the fast-evolving understanding of isoprene

photooxidation. This knowledge is needed to predict nitrogen and ozone budgets in this region and elsewhere in the world with similar photochemical environments. Here we use extensive aircraft and ground observations, combined with a global chemistry-climate model (GFDL AM3), to examine decadal changes in NO_y abundance and speciation as well as in surface O_3 mixing ratios over the Southeast U.S. between the summers of 2004 and 2013. We then use the model to infer future NO_y speciation and surface ozone abundances in response to further NO_x emission controls in this region.

We first evaluate the model with aircraft and surface observations. When we apply the estimated 40 % reductions in anthropogenic NO_x emissions from 2004 to 2013, our model reproduces the vertical profiles of NO_x, HNO_3, PAN, ∑ANs and NO_y observed during aircraft campaigns over the Southeast U.S. in the summers of 2004 and 2013. By including recent updates on isoprene oxidation, our model can largely reproduce the vertical profiles of ∑ANs and several speciated alkyl nitrates, as well as their correlations with O_x and HCHO (Figure 4), lending support to the model representation of isoprene oxidation. On the other hand, we show that the discrepancy between measured ∑ANs and speciated $RONO_2$, can be explained by a combination of terpene nitrates, dinitrates and nighttime NO_3 oxidation products from isoprene. We also show that modeled ozone appears to be insensitive to hydrolysis of ISOPNB, because its photooxidation, mainly by OH, also returns little NO_x.

Major NO_y species decline proportionally as a result of NO_x emission reductions in the Southeast U.S., except that ∑ANs decline at a slower rate. Our model suggests that summertime monthly averaged NO_x, HNO_3, PAN, and NO_y decline by 30-40 %, in response to 40 % reductions in anthropogenic NO_x emissions from 2004 to 2013. The slower decline of ∑ANs reflects the prolonged lifetime of NO_x with decreasing NO_x. This proportional decrease is to a large extent driven by high concentrations of biogenic VOC in this region that change little in magnitude from 2004 to 2013. In contrast, Pollack et al. (2013) find a faster PAN decrease than HNO_3 in the LA basin over the past several decades, partly due to the decrease in anthropogenic VOC emissions that are major PAN precursors.

Deposited and exported NO_y decline with NO_x emission reductions. The model also shows a decrease of NO_3^- wet deposition flux by 29 % from 2004 to 2013, consistent with observations from the NADP network (- 24 %). We find from model calculations that the NO_y export efficiency remains at 12 % in both 2004 and 2013, leading to a proportional decrease of exported NO_y. The dominant NO_y export terms include NO_x or HNO_3, each accounting for 6% of the total exported NO_y, followed by ∑PNs (4 %) and ∑ANs (2 %).

Response of surface ozone to NO_x emission reductions reveals a strong O_3-NO_x sensitivity in summertime over Southeast U.S. Observations from EPA AQS surface

network suggest that mean MDA8 ozone during July-August has decreased from 48 ppb in 2004 to 37 ppb in 2013, a 23 % decrease. Despite a positive bias of upto 12 ppb in boundary layer ozone and a bias of 16 ppb in surface MDA8 ozone, our model shows a 10 ppb decrease of surface MDA8 ozone from 2004 to 2013, very close to the observed 11 ppb decrease from the EPA data. The bias of ozone in our model is not entirely attributed to uncertainties in NO_x emissions, as the overestimate suggested by earlier work would lead to underestimate of NO_y. More importantly, we find from model calculations that modeled MDA8 O_3 will continue to decrease by another 9 ppb assuming anthropogenic NO_x emissions are decreased by 40 % from the 2013 level with meteorology and other emissions kept constant. In addition, further NO_x reduction leads to less frequent extreme ozone events (Figure 7). This continued strong sensitivity of surface O_3 to NO_x emissions can guide the development effective emission control strategies for improving future air quality.

Data availability

Observational datasets and modeling results are available upon request to the corresponding author (jmao2@alaska.edu).

Author contributions

This was largely a collaborative effort. R. C. Cohen, J. D. Crounse, A. P. Teng, P. O. Wennberg, B. H. Lee, F. D. Lopez-Hilfiker, J. A. Thornton, J. Peischl, I. B. Pollack, T. B. Ryerson, P. Veres, J. M. Roberts, A. Neuman, J. B. Nowak, G. M. Wolfe, T. F. Hanisco, A. Fried, H. B. Singh, J. Dibb contributed to the collection of aircraft observations in 2004 and 2013; J.Mao and J.Li conceived the study; J.Li and J. Mao performed analysis and modeling; J.Li, J.Mao, A. M. Fiore, R. C. Cohen, P. O. Wennberg, J. D. Crounse, J. A. Thornton, A. Neuman, J. B. Nowak, J. Peischl, J. Dibb, F. Paulot, L. W. Horowitz and G. M. Wolfe wrote the paper with input from all coauthors.

Competing interests

The authors declare that they have no conflict of interest.

Acknowledgements

The authors thank Vaishali Naik (NOAA GFDL) for providing emission inventories in the GFDL AM3 model, and Leo Donner (NOAA GFDL) and William Cooke (UCAR/NOAA) for the help with convection scheme of AM3. J.L., J.M. and L.W.H. acknowledge support from the NOAA Climate Program Office grant # NA13OAR431007. J.M., L.W.H. and A.M.F. acknowledge support from NOAA Climate Program Office grant #NA14OAR4310133. J.D.C. and P.O.W. acknowledge support from NASA grants (NNX12AC06G and NNX14AP46G). J.L acknowledge support from the Startup Foundation for Introducing Talent of NUIST grant #2243141701014 and the

Priority Academic Program Development of Jiangsu Higher Education Institutions (PAPD).

References

Ahmadov, R., McKeen, S., Trainer, M., Banta, R., Brewer, A., Brown, S., Edwards, P. M., de Gouw, J. A., Frost, G. J., Gilman, J., Helmig, D., Johnson, B., Karion, A., Koss, A., Langford, A., Lerner, B., Olson, J., Oltmans, S., Peischl, J., Pétron, G., Pichugina, Y., Roberts, J. M., Ryerson, T., Schnell, R., Senff, C., Sweeney, C., Thompson, C., Veres, P. R., Warneke, C., Wild, R., Williams, E. J., Yuan, B., and Zamora, R.: Understanding high wintertime ozone pollution events in an oil- and natural gas-producing region of the western US, Atmos. Chem. Phys., 15, 1, 411-429, 2015.

Anderson, D. C., Loughner, C. P., Diskin, G., Weinheimer, A., Canty, T. P., Salawitch, R. J., Worden, H. M., Fried, A., Mikoviny, T., Wisthaler, A., and Dickerson, R. R.: Measured and modeled CO and NOy in DISCOVER-AQ: An evaluation of emissions and chemistry over the eastern US, Atmos. Environ., 96, 78-87, 2014.

Appel, K., Foley, K., Bash, J., Pinder, R., Dennis, R., Allen, D., and Pickering, K.: A multi-resolution assessment of the Community Multiscale Air Quality (CMAQ) model v4. 7 wet deposition estimates for 2002–2006, Geosci. Model. Dev., 4, 2, 357-371, 2011.

Aschmann, S. M., Atkinson, R., and Arey, J.: Products of reaction of OH radicals with α - pinene, J. Geophys. Res., 107, D14, 2002.

Ayres, B. R., Allen, H. M., Draper, D. C., Brown, S. S., Wild, R. J., Jimenez, J. L., Day, D. A., Campuzano-Jost, P., Hu, W., de Gouw, J., Koss, A., Cohen, R. C., Duffey, K. C., Romer, P., Baumann, K., Edgerton, E., Takahama, S., Thornton, J. A., Lee, B. H., Lopez-Hilfiker, F. D., Mohr, C., Wennberg, P. O., Nguyen, T. B., Teng, A., Goldstein, A. H., Olson, K., and Fry, J. L.: Organic nitrate aerosol formation via NO3 + biogenic volatile organic compounds in the southeastern United States, Atmos. Chem. Phys., 15, 23, 13377-13392, 2015.

Bates, K. H., Crounse, J. D., St. Clair, J. M., Bennett, N. B., Nguyen, T. B., Seinfeld, J. H., Stoltz, B. M., and Wennberg, P. O.: Gas Phase Production and Loss of Isoprene Epoxydiols, J. Phys. Chem. A, 118, 7, 1237-1246, 2014.

Bates, K. H., Nguyen, T. B., Teng, A. P., Crounse, J. D., Kjaergaard, H. G., Stoltz, B. M., Seinfeld, J. H., and Wennberg, P. O.: Production and Fate of C4 Dihydroxycarbonyl Compounds from Isoprene Oxidation, J. Phys. Chem. A, 120, 1, 106-117, 2016.

Bean, J. K., and Hildebrandt Ruiz, L.: Gas–particle partitioning and hydrolysis of organic nitrates formed from the oxidation of α-pinene in environmental chamber experiments, Atmos. Chem. Phys., 16, 4, 2175-2184, 2016.

Bloomer, B. J., Vinnikov, K. Y., and Dickerson, R. R.: Changes in seasonal and diurnal cycles of ozone and temperature in the eastern U.S, Atmos. Environ., 44, 21–22, 2543-2551, 2010.

Boyd, C. M., Sanchez, J., Xu, L., Eugene, A. J., Nah, T., Tuet, W. Y., Guzman, M. I., and Ng, N. L.: Secondary organic aerosol formation from the β-pinene+NO3 system: effect of humidity and peroxy radical fate, Atmos. Chem. Phys., 15, 13, 7497-7522, 2015.

Brown-Steiner, B., Hess, P. G., and Lin, M. Y.: On the capabilities and limitations of GCCM simulations of summertime regional air quality: A diagnostic analysis of ozone and temperature simulations in the US using CESM CAM-Chem, Atmos. Environ., 101, 134-148, 2015.

Browne, E. C., and Cohen, R. C.: Effects of biogenic nitrate chemistry on the NOx lifetime in remote continental regions, Atmos. Chem. Phys., 12, 24, 11917-11932, 2012.

Browne, E. C., Wooldridge, P. J., Min, K. E., and Cohen, R. C.: On the role of monoterpene chemistry in the remote continental boundary layer, Atmos. Chem. Phys., 14, 3, 1225-1238, 2014.

Camalier, L., Cox, W., and Dolwick, P.: The effects of meteorology on ozone in urban areas and their use in assessing ozone trends, Atmos. Environ., 41, 33, 7127-7137, 2007.

Canty, T. P., Hembeck, L., Vinciguerra, T. P., Anderson, D. C., Goldberg, D. L., Carpenter, S. F., Allen, D. J., Loughner, C. P., Salawitch, R. J., and Dickerson, R. R.: Ozone and NOx chemistry in the eastern US: evaluation of CMAQ/CB05 with satellite (OMI) data, Atmos. Chem. Phys., 15, 4, 4427-4461, 2015.

Cooper, O. R., Gao, R.-S., Tarasick, D., Leblanc, T., and Sweeney, C.: Long-term ozone trends at rural ozone monitoring sites across the United States, 1990–2010, J. Geophys. Res., 117, D22307, 2012.

Crounse, J. D., Paulot, F., Kjaergaard, H. G., and Wennberg, P. O.: Peroxy radical isomerization in the oxidation of isoprene, Phys. Chem. Chem. Phys., 13, 30, 13607-13613, 2011.

Darer, A. I., Cole-Filipiak, N. C., O'Connor, A. E., and Elrod, M. J.: Formation and Stability of Atmospherically Relevant Isoprene-Derived Organosulfates and Organonitrates, Environ. Sci. Technol., 45, 5, 1895-1902, 2011.

Donner, L. J., Wyman, B. L., Hemler, R. S., Horowitz, L. W., Ming, Y., Zhao, M., Golaz, J.-C., Ginoux, P., Lin, S.-J., Schwarzkopf, M. D., Austin, J., Alaka, G., Cooke, W. F., Delworth, T. L., Freidenreich, S. M., Gordon, C. T., Griffies, S. M., Held, I. M., Hurlin, W. J., Klein, S. A., Knutson, T. R., Langenhorst, A. R., Lee, H.-C., Lin, Y., Magi, B. I., Malyshev, S. L., Milly, P. C. D., Naik, V., Nath, M. J., Pincus, R., Ploshay, J. J., Ramaswamy, V., Seman, C. J., Shevliakova, E., Sirutis, J. J., Stern, W. F., Stouffer, R. J., Wilson, R. J., Winton, M., Wittenberg, A. T., and Zeng, F.: The Dynamical Core, Physical Parameterizations, and Basic Simulation Characteristics of the Atmospheric Component AM3 of the GFDL Global Coupled Model CM3, J. Climate, 24, 13, 3484-3519, 2011.

Fang, Y., Fiore, A. M., Horowitz, L., Levy, H., Hu, Y., and Russell, A.: Sensitivity of the NOy budget over the United States to anthropogenic and lightning NOx in summer, J. Geophys. Res., 115, D18, 2010.

Fehsenfeld, F. C., Ancellet, G., Bates, T. S., Goldstein, A. H., Hardesty, R. M., Honrath, R., Law, K. S., Lewis, A. C., Leaitch, R., McKeen, S., Meagher, J., Parrish, D. D., Pszenny, A. A. P., Russell, P. B., Schlager, H., Seinfeld, J., Talbot, R., and Zbinden, R.: International Consortium for Atmospheric Research on Transport and Transformation (ICARTT): North America to Europe—Overview of the 2004 summer field study, J. Geophys. Res., 111, D23S01, 2006.

Fiore, A. M., Horowitz, L. W., Purves, D. W., Levy, H., Evans, M. J., Wang, Y., Li, Q., and Yantosca, R. M.: Evaluating the contribution of changes in isoprene emissions to surface ozone trends over the eastern United States, J. Geophys. Res., 110, D12303, 2005.

Fiore, A. M., Dentener, F. J., Wild, O., Cuvelier, C., Schultz, M. G., Hess, P., Textor, C., Schulz, M., Doherty, R. M., and Horowitz, L. W.: Multimodel estimates of intercontinental source - receptor relationships for ozone pollution, J. Geophys. Res., 114, D4, 83-84, 2009.

Fischer, E., Jacob, D. J., Yantosca, R. M., Sulprizio, M. P., Millet, D., Mao, J., Paulot, F., Singh, H., Roiger, A., and Ries, L.: Atmospheric peroxyacetyl nitrate (PAN): a global budget and source attribution, Atmos. Chem. Phys., 14, 5, 2679-2698, 2014.

Fisher, J. A., Jacob, D. J., Travis, K. R., Kim, P. S., Marais, E. A., Miller, C. C., Yu, K., Zhu, L., Yantosca, R. M., and Sulprizio, M. P.: Organic nitrate chemistry and its implications for nitrogen budgets in an isoprene- and monoterpene-rich atmosphere: constraints from aircraft (SEAC4RS) and ground-based (SOAS) observations in the Southeast US, Atmos. Chem. Phys., 16, 1, 1-38, 2016.

Fry, J. L., Kiendler-Scharr, A., Rollins, A. W., Wooldridge, P. J., Brown, S. S., Fuchs, H., Dubé, W., Mensah, A., dal Maso, M., Tillmann, R., Dorn, H. P., Brauers, T., and Cohen, R. C.: Organic nitrate and secondary organic aerosol yield from NO3 oxidation of β-pinene evaluated using a gas-phase kinetics/aerosol partitioning model, Atmos. Chem. Phys., 9, 4, 1431-1449, 2009.

Fry, J. L., Draper, D. C., Barsanti, K. C., Smith, J. N., Ortega, J., Winkler, P. M., Lawler, M. J., Brown, S. S., Edwards, P. M., Cohen, R. C., and Lee, L.: Secondary Organic Aerosol Formation and Organic Nitrate Yield from NO3 Oxidation of Biogenic Hydrocarbons, Environ. Sci. Technol., 48, 20, 11944-11953, 2014.

Granier, C., Bessagnet, B., Bond, T., D'Angiola, A., Denier van der Gon, H., Frost, G. J., Heil, A., Kaiser, J. W., Kinne, S., Klimont, Z., Kloster, S., Lamarque, J.-F., Liousse, C., Masui, T., Meleux, F., Mieville, A., Ohara, T., Raut, J.-C., Riahi, K., Schultz, M. G., Smith, S. J., Thompson, A., van Aardenne, J., van der Werf, G. R., and van Vuuren, D. P.: Evolution of anthropogenic and biomass burning emissions of air pollutants at global and regional scales during the 1980–2010 period, Clim. Change, 109, 1, 163-190, 2011.

Grimm, J. W., and Lynch, J. A.: Improved daily precipitation nitrate and ammonium concentration models for the Chesapeake Bay Watershed, Environ. Pollut., 135, 3, 445-455, 2005.

Hardacre, C., Wild, O., and Emberson, L.: An evaluation of ozone dry deposition in global scale chemistry climate models, Atmos. Chem. Phys., 15, 11, 6419-6436, 2015.

Henderson, B. H., Pinder, R. W., Crooks, J., Cohen, R. C., Hutzell, W. T., Sarwar, G., Goliff, W. S., Stockwell, W. R., Fahr, A., Mathur, R., Carlton, A. G., and Vizuete, W.: Evaluation of simulated photochemical partitioning of oxidized nitrogen in the upper troposphere, Atmos. Chem. Phys., 11, 1, 275-291, 2011.

Hidy, G. M., Blanchard, C. L., Baumann, K., Edgerton, E., Tanenbaum, S., Shaw, S., Knipping, E., Tombach, I., Jansen, J., and Walters, J.: Chemical climatology of the southeastern United States, 1999–2013, Atmos. Chem. Phys., 14, 21, 11893-11914, 2014.

Hidy, G. M., and Blanchard, C. L.: Precursor reductions and ground-level ozone in the Continental United States, J. Air Waste Manag. Assoc., 65, 10, 1261-1282, 2015.

Horowitz, L. W., Liang, J., Gardner, G. M., and Jacob, D. J.: Export of reactive nitrogen from North America during summertime: Sensitivity to hydrocarbon chemistry, J. Geophys. Res., 103, D11, 13451-13476, 1998.

Horowitz, L. W., Fiore, A. M., Milly, G. P., Cohen, R. C., Perring, A., Wooldridge, P. J., Hess, P. G., Emmons, L. K., and Lamarque, J.-F.: Observational constraints on the chemistry of isoprene nitrates over the eastern United States, J. Geophys. Res., 112, D12S08, 2007.

Hu, K. S., Darer, A. I., and Elrod, M. J.: Thermodynamics and kinetics of the hydrolysis of atmospherically relevant organonitrates and organosulfates, Atmos. Chem. Phys., 11, 16, 8307-8320, 2011.

Hudman, R., Jacob, D. J., Cooper, O., Evans, M., Heald, C., Park, R., Fehsenfeld, F., Flocke, F., Holloway, J., and Hübler, G.: Ozone production in transpacific Asian pollution plumes and implications for ozone air quality in California, J. Geophys. Res., 109, D23, 2004.

Hudman, R. C., Jacob, D. J., Turquety, S., Leibensperger, E. M., Murray, L. T., Wu, S., Gilliland, A. B., Avery, M., Bertram, T. H., Brune, W., Cohen, R. C., Dibb, J. E., Flocke, F. M., Fried, A., Holloway, J., Neuman, J. A., Orville, R., Perring, A., Ren, X., Sachse, G. W., Singh, H. B., Swanson, A., and Wooldridge, P. J.: Surface and lightning sources of nitrogen oxides over the United States: Magnitudes, chemical evolution, and outflow, J. Geophys. Res., 112, D12S05, 2007.

Hudman, R. C., Moore, N. E., Mebust, A. K., Martin, R. V., Russell, A. R., Valin, L. C., and Cohen, R. C.: Steps towards a mechanistic model of global soil nitric oxide

emissions: implementation and space based-constraints, Atmos. Chem. Phys., 12, 16, 7779-7795, 2012.

Ito, A., Sillman, S., and Penner, J. E.: Global chemical transport model study of ozone response to changes in chemical kinetics and biogenic volatile organic compounds emissions due to increasing temperatures: Sensitivities to isoprene nitrate chemistry and grid resolution, J. Geophys. Res., 114, D09301, 2009.

Jacob, D. J., Logan, J. A., Gardner, G. M., Yevich, R. M., Spivakovsky, C. M., Wofsy, S. C., Sillman, S., and Prather, M. J.: Factors regulating ozone over the United States and its export to the global atmosphere, J. Geophys. Res., 98, D8, 1993.

Jacob, D. J., and Winner, D. A.: Effect of climate change on air quality, Atmos. Environ., 43, 1, 51-63, 2009.

Jacobs, M. I., Burke, W. J., and Elrod, M. J.: Kinetics of the reactions of isoprene-derived hydroxynitrates: gas phase epoxide formation and solution phase hydrolysis, Atmos. Chem. Phys., 14, 17, 8933-8946, 2014.

Jenkin, M. E., Young, J. C., and Rickard, A. R.: The MCM v3.3.1 degradation scheme for isoprene, Atmos. Chem. Phys., 15, 20, 11433-11459, 2015.

Kavassalis, S., and Murphy, J. G.: Understanding ozone-meteorology correlations: a role for dry deposition, Geophys. Res. Lett.10.1002/2016GL071791, 2017.

Krotkov, N. A., McLinden, C. A., Li, C., Lamsal, L. N., Celarier, E. A., Marchenko, S. V., Swartz, W. H., Bucsela, E. J., Joiner, J., Duncan, B. N., Boersma, K. F., Veefkind, J. P., Levelt, P. F., Fioletov, V. E., Dickerson, R. R., He, H., Lu, Z., and Streets, D. G.: Aura OMI observations of regional SO2 and NO2 pollution changes from 2005 to 2015, Atmos. Chem. Phys., 16, 7, 4605-4629, 2016.

Lam, Y., Fu, J., Wu, S., and Mickley, L.: Impacts of future climate change and effects of biogenic emissions on surface ozone and particulate matter concentrations in the United States, Atmos. Chem. Phys., 11, 10, 4789-4806, 2011.

Lamarque, J.-F., Kyle, G. P., Meinshausen, M., Riahi, K., Smith, S. J., van Vuuren, D. P., Conley, A. J., and Vitt, F.: Global and regional evolution of short-lived radiatively-active gases and aerosols in the Representative Concentration Pathways, Clim. Change, 109, 1, 191-212, 2011.

Lamsal, L. N., Duncan, B. N., Yoshida, Y., Krotkov, N. A., Pickering, K. E., Streets, D. G., and Lu, Z.: U.S. NO2 trends (2005–2013): EPA Air Quality System (AQS) data versus improved observations from the Ozone Monitoring Instrument (OMI), Atmos. Environ., 110, 130-143, 2015.

Lee, B. H., Mohr, C., Lopez-Hilfiker, F. D., Lutz, A., Hallquist, M., Lee, L., Romer, P., Cohen, R. C., Iyer, S., Kurtén, T., Hu, W., Day, D. A., Campuzano-Jost, P., Jimenez, J. L., Xu, L., Ng, N. L., Guo, H., Weber, R. J., Wild, R. J., Brown, S. S., Koss, A., de Gouw,

J., Olson, K., Goldstein, A. H., Seco, R., Kim, S., McAvey, K., Shepson, P. B., Starn, T., Baumann, K., Edgerton, E. S., Liu, J., Shilling, J. E., Miller, D. O., Brune, W., Schobesberger, S., D'Ambro, E. L., and Thornton, J. A.: Highly functionalized organic nitrates in the southeast United States: Contribution to secondary organic aerosol and reactive nitrogen budgets, Proc. Natl. Acad. Sci. U.S.A., 113, 6, 1516-1521, 2016.

Lee, L., Teng, A. P., Wennberg, P. O., Crounse, J. D., and Cohen, R. C.: On Rates and Mechanisms of OH and O3 Reactions with Isoprene-Derived Hydroxy Nitrates, J. Phys. Chem. A, 118, 9, 1622-1637, 2014.

Li, J., Mao, J., Min, K.-E., Washenfelder, R. A., Brown, S. S., Kaiser, J., Keutsch, F. N., Volkamer, R., Wolfe, G. M., Hanisco, T. F., Pollack, I. B., Ryerson, T. B., Graus, M., Gilman, J. B., Lerner, B. M., Warneke, C., de Gouw, J. A., Middlebrook, A. M., Liao, J., Welti, A., Henderson, B. H., McNeill, V. F., Hall, S. R., Ullmann, K., Donner, L. J., Paulot, F., and Horowitz, L. W.: Observational constraints on glyoxal production from isoprene oxidation and its contribution to organic aerosol over the Southeast United States, J. Geophys. Res., 121, 16, 2016JD025331, 2016.

Li, Q., Jacob, D. J., Munger, J. W., Yantosca, R. M., and Parrish, D. D.: Export of NOy from the North American boundary layer: Reconciling aircraft observations and global model budgets, J. Geophys. Res., 109, D2, 2004.

Liang, J., Horowitz, L. W., Jacob, D. J., Wang, Y., Fiore, A. M., Logan, J. A., Gardner, G. M., and Munger, J. W.: Seasonal budgets of reactive nitrogen species and ozone over the United States, and export fluxes to the global atmosphere, J. Geophys. Res., 103, D11, 13435-13450, 1998.

Lin, M., Horowitz, L. W., Payton, R., Fiore, A. M., and Tonnesen, G.: US surface ozone trends and extremes from 1980 to 2014: quantifying the roles of rising Asian emissions, domestic controls, wildfires, and climate, Atmos. Chem. Phys., 17, 4, 2943-2970, 2017.

Lockwood, A. L., Shepson, P. B., Fiddler, M. N., and Alaghmand, M.: Isoprene nitrates: preparation, separation, identification, yields, and atmospheric chemistry, Atmos. Chem. Phys., 10, 13, 6169-6178, 2010.

Lu, Z., Streets, D. G., De Foy, B., Lamsal, L. N., Duncan, B. N., and Xing, J.: Emissions of nitrogen oxides from US urban areas: estimation from Ozone Monitoring Instrument retrievals for 2005-2014, Atmos. Chem. Phys., 15, 10, 14961-15003, 2015.

Mao, J., Paulot, F., Jacob, D. J., Cohen, R. C., Crounse, J. D., Wennberg, P. O., Keller, C. A., Hudman, R. C., Barkley, M. P., and Horowitz, L. W.: Ozone and organic nitrates over the eastern United States: Sensitivity to isoprene chemistry, J. Geophys. Res., 118, 19, 11,256-211,268, 2013.

Marais, E. A., Jacob, D. J., Jimenez, J. L., Campuzano-Jost, P., Day, D. A., Hu, W., Krechmer, J., Zhu, L., Kim, P. S., Miller, C. C., Fisher, J. A., Travis, K., Yu, K., Hanisco, T. F., Wolfe, G. M., Arkinson, H. L., Pye, H. O. T., Froyd, K. D., Liao, J., and McNeill, V. F.: Aqueous-phase mechanism for secondary organic aerosol formation from isoprene:

application to the southeast United States and co-benefit of SO2 emission controls, Atmos. Chem. Phys., 16, 3, 1603-1618, 2016.

Metcalfe, S. E., Whyatt, J. D., Nicholson, J. P. G., Derwent, R. G., and Heywood, E.: Issues in model validation: assessing the performance of a regional-scale acid deposition model using measured and modelled data, Atmos. Environ., 39, 4, 587-598, 2005.

Millet, D. B., Jacob, D. J., Boersma, K. F., Fu, T. M., Kurosu, T. P., Chance, K., Heald, C. L., and Guenther, A.: Spatial Distribution of Isoprene Emissions from North America Derived from Dormaldehyde Column Measurements by the OMI Satellite Sensor, J. Geophys. Res., 113, D2, 194-204, 2008.

Miyazaki, K., Eskes, H., Sudo, K., Boersma, K. F., Bowman, K., and Kanaya, Y.: Decadal changes in global surface NOx emissions from multi-constituent satellite data assimilation, Atmos. Chem. Phys., 17, 2, 807-837, 2017.

Moxim, W., Levy, H., and Kasibhatla, P.: Simulated global tropospheric PAN: Its transport and impact on NO x, J. Geophys. Res., 101, D7, 12621-12638, 1996.

Müller, J. F., Peeters, J., and Stavrakou, T.: Fast photolysis of carbonyl nitrates from isoprene, Atmos. Chem. Phys., 14, 5, 2497-2508, 2014.

Nah, T., Sanchez, J., Boyd, C. M., and Ng, N. L.: Photochemical Aging of α-pinene and β-pinene Secondary Organic Aerosol formed from Nitrate Radical Oxidation, Environ. Sci. Technol., 50, 1, 222-231, 2016.

Naik, V., Horowitz, L. W., Fiore, A. M., Ginoux, P., Mao, J., Aghedo, A. M., and Levy, H.: Impact of preindustrial to present-day changes in short-lived pollutant emissions on atmospheric composition and climate forcing, J. Geophys. Res., 118, 14, 8086-8110, 2013.

Neuman, J., Parrish, D., Trainer, M., Ryerson, T., Holloway, J., Nowak, J., Swanson, A., Flocke, F., Roberts, J., and Brown, S.: Reactive nitrogen transport and photochemistry in urban plumes over the North Atlantic Ocean, J. Geophys. Res., 111, D23, 2006.

Ng, N. L., Kwan, A. J., Surratt, J. D., Chan, A. W. H., Chhabra, P. S., Sorooshian, A., Pye, H. O. T., Crounse, J. D., Wennberg, P. O., Flagan, R. C., and Seinfeld, J. H.: Secondary organic aerosol (SOA) formation from reaction of isoprene with nitrate radicals (NO3), Atmos. Chem. Phys., 8, 14, 4117-4140, 2008.

Nguyen, T. B., Crounse, J. D., Teng, A. P., St. Clair, J. M., Paulot, F., Wolfe, G. M., and Wennberg, P. O.: Rapid deposition of oxidized biogenic compounds to a temperate forest, Proc. Natl. Acad. Sci. U.S.A., 112, 5, E392-E401, 2015.

Nozière, B., Barnes, I., and Becker, K. H.: Product study and mechanisms of the reactions of α - pinene and of pinonaldehyde with OH radicals, J. Geophys. Res., 104, D19, 23645-23656, 1999.

Palmer, P. I., Jacob, D. J., Fiore, A. M., Martin, R. V., Chance, K., and Kurosu, T. P.: Mapping isoprene emissions over North America using formaldehyde column observations from space, J. Geophys. Res., 108, D6, 2003.

Parrish, D., Ryerson, T., Holloway, J., Neuman, J., Roberts, J., Williams, J., Stroud, C., Frost, G., Trainer, M., and Hübler, G.: Fraction and composition of NOy transported in air masses lofted from the North American continental boundary layer, J. Geophys. Res., 109, D9, 2004.

Paulot, F., Crounse, J. D., Kjaergaard, H. G., Kroll, J. H., Seinfeld, J. H., and Wennberg, P. O.: Isoprene photooxidation: new insights into the production of acids and organic nitrates, Atmos. Chem. Phys., 9, 4, 1479-1501, 2009.

Paulot, F., Henze, D. K., and Wennberg, P. O.: Impact of the isoprene photochemical cascade on tropical ozone, Atmos. Chem. Phys., 12, 3, 1307-1325, 2012.

Paulot, F., Jacob, D. J., Pinder, R. W., Bash, J. O., Travis, K., and Henze, D. K.: Ammonia emissions in the United States, European Union, and China derived by high-resolution inversion of ammonium wet deposition data: Interpretation with a new agricultural emissions inventory (MASAGE_NH3), J. Geophys. Res., 119, 7, 4343-4364, 2014.

Paulot, F., Ginoux, P., Cooke, W. F., Donner, L. J., Fan, S., Lin, M. Y., Mao, J., Naik, V., and Horowitz, L. W.: Sensitivity of nitrate aerosols to ammonia emissions and to nitrate chemistry: implications for present and future nitrate optical depth, Atmos. Chem. Phys., 16, 3, 1459-1477, 2016.

Peeters, J., Müller, J.-F., Stavrakou, T., and Nguyen, V. S.: Hydroxyl Radical Recycling in Isoprene Oxidation Driven by Hydrogen Bonding and Hydrogen Tunneling: The Upgraded LIM1 Mechanism, J. Phys. Chem. A, 118, 38, 8625-8643, 2014.

Perring, A. E., Pusede, S. E., and Cohen, R. C.: An Observational Perspective on the Atmospheric Impacts of Alkyl and Multifunctional Nitrates on Ozone and Secondary Organic Aerosol, Chem. Rev., 113, 8, 5848-5870, 2013.

Pollack, I. B., Ryerson, T. B., Trainer, M., Neuman, J., Roberts, J. M., and Parrish, D. D.: Trends in ozone, its precursors, and related secondary oxidation products in Los Angeles, California: A synthesis of measurements from 1960 to 2010, J. Geophys. Res., 118, 11, 5893-5911, 2013.

Praske, E., Crounse, J. D., Bates, K. H., Kurtén, T., Kjaergaard, H. G., and Wennberg, P. O.: Atmospheric Fate of Methyl Vinyl Ketone: Peroxy Radical Reactions with NO and HO2, J. Phys. Chem. A, 119, 19, 4562-4572, 2015.

Price, C., Penner, J., and Prather, M.: NOx from lightning: 1. Global distribution based on lightning physics, J. Geophys. Res., 102, D5, 5929-5941, 1997.

Pye, H. O. T., Luecken, D. J., Xu, L., Boyd, C. M., Ng, N. L., Baker, K. R., Ayres, B. R., Bash, J. O., Baumann, K., Carter, W. P. L., Edgerton, E., Fry, J. L., Hutzell, W. T., Schwede, D. B., and Shepson, P. B.: Modeling the Current and Future Roles of Particulate Organic Nitrates in the Southeastern United States, Environ. Sci. Technol., 49, 24, 14195-14203, 2015.

Rieder, H. E., Fiore, A. M., Horowitz, L. W., and Naik, V.: Projecting policy - relevant metrics for high summertime ozone pollution events over the eastern United States due to climate and emission changes during the 21st century, J. Geophys. Res., 120, 2, 784-800, 2015.

Rindelaub, J. D., McAvey, K. M., and Shepson, P. B.: The photochemical production of organic nitrates from α-pinene and loss via acid-dependent particle phase hydrolysis, Atmos. Environ., 100, 193-201, 2015.

Rollins, A. W., Kiendler-Scharr, A., Fry, J. L., Brauers, T., Brown, S. S., Dorn, H. P., Dubé, W. P., Fuchs, H., Mensah, A., Mentel, T. F., Rohrer, F., Tillmann, R., Wegener, R., Wooldridge, P. J., and Cohen, R. C.: Isoprene oxidation by nitrate radical: alkyl nitrate and secondary organic aerosol yields, Atmos. Chem. Phys., 9, 18, 6685-6703, 2009.

Rollins, A. W., Smith, J. D., Wilson, K. R., and Cohen, R. C.: Real Time In Situ Detection of Organic Nitrates in Atmospheric Aerosols, Environ. Sci. Technol., 44, 14, 5540-5545, 2010.

Romer, P. S., Duffey, K. C., Wooldridge, P. J., Allen, H. M., Ayres, B. R., Brown, S. S., Brune, W. H., Crounse, J. D., de Gouw, J., Draper, D. C., Feiner, P. A., Fry, J. L., Goldstein, A. H., Koss, A., Misztal, P. K., Nguyen, T. B., Olson, K., Teng, A. P., Wennberg, P. O., Wild, R. J., Zhang, L., and Cohen, R. C.: The lifetime of nitrogen oxides in an isoprene-dominated forest, Atmos. Chem. Phys., 16, 12, 7623-7637, 2016.

Russell, A. R., Valin, L. C., and Cohen, R. C.: Trends in OMI NO2 observations over the United States: effects of emission control technology and the economic recession, Atmos. Chem. Phys., 12, 24, 12197-12209, 2012.

Sanderson, M., Dentener, F., Fiore, A., Cuvelier, C., Keating, T., Zuber, A., Atherton, C., Bergmann, D., Diehl, T., and Doherty, R.: A multi - model study of the hemispheric transport and deposition of oxidised nitrogen, Geophys. Res. Lett., 35, 17, 2008.

Sato, K.: Detection of nitrooxypolyols in secondary organic aerosol formed from the photooxidation of conjugated dienes under high-NOx conditions, Atmos. Environ., 42, 28, 6851-6861, 2008.

Schwantes, R. H., Teng, A. P., Nguyen, T. B., Coggon, M. M., Crounse, J. D., St. Clair, J. M., Zhang, X., Schilling, K. A., Seinfeld, J. H., and Wennberg, P. O.: Isoprene NO3 Oxidation Products from the RO2 + HO2 Pathway, J. Phys. Chem. A, 119, 40, 10158-10171, 2015.

Sillman, S.: Ozone production efficiency and loss of NO x in power plant plumes: Photochemical model and interpretation of measurements in Tennessee, J. Geophys. Res., 105, D7, 9189-9202, 2000.

Simon, H., Reff, A., Wells, B., Xing, J., and Frank, N.: Ozone Trends Across the United States over a Period of Decreasing NOx and VOC Emissions, Environ. Sci. Technol., 49, 1, 186-195, 2015.

Singh, H. B., Brune, W. H., Crawford, J. H., Jacob, D. J., and Russell, P. B.: Overview of the summer 2004 Intercontinental Chemical Transport Experiment–North America (INTEX-A), J. Geophys. Res., 111, D24S01, 2006.

Souri, A. H., Choi, Y., Jeon, W., Li, X., Pan, S., Diao, L., and Westenbarger, D. A.: Constraining NOx emissions using satellite NO2 measurements during 2013 DISCOVER-AQ Texas campaign, Atmos. Environ., 131, 371-381, 2016.

Spittler, M., Barnes, I., Bejan, I., Brockmann, K. J., Benter, T., and Wirtz, K.: Reactions of NO3 radicals with limonene and α-pinene: Product and SOA formation, Atmos. Environ., 40, 116-127, 2006.

St. Clair, J. M., Rivera-Rios, J. C., Crounse, J. D., Knap, H. C., Bates, K. H., Teng, A. P., Jørgensen, S., Kjaergaard, H. G., Keutsch, F. N., and Wennberg, P. O.: Kinetics and Products of the Reaction of the First-Generation Isoprene Hydroxy Hydroperoxide (ISOPOOH) with OH, J. Phys. Chem. A, 120, 9, 1441-1451, 2016.

Steiner, A. L., Davis, A. J., Sillman, S., Owen, R. C., Michalak, A. M., and Fiore, A. M.: Observed suppression of ozone formation at extremely high temperatures due to chemical and biophysical feedbacks, Proc. Natl. Acad. Sci. U.S.A., 107, 46, 19685-19690, 2010.

Stoeckenius, T. E., Hogrefe, C., Zagunis, J., Sturtz, T. M., Wells, B., and Sakulyanontvittaya, T.: A comparison between 2010 and 2006 air quality and meteorological conditions, and emissions and boundary conditions used in simulations of the AQMEII-2 North American domain, Atmos. Environ., 115, 389-403, 2015.

Stohl, A., Trainer, M., Ryerson, T. B., Holloway, J. S., and Parrish, D. D.: Export of NOy from the North American boundary layer during 1996 and 1997 North Atlantic Regional Experiments, J. Geophys. Res., 107, D11, ACH 11-11-ACH 11-13, 2002.

Strode, S. A., Rodriguez, J. M., Logan, J. A., Cooper, O. R., Witte, J. C., Lamsal, L. N., Damon, M., Van Aartsen, B., Steenrod, S. D., and Strahan, S. E.: Trends and variability in surface ozone over the United States, J. Geophys. Res., 120, 17, 9020-9042, 2015.

Szmigielski, R., Vermeylen, R., Dommen, J., Metzger, A., Maenhaut, W., Baltensperger, U., and Claeys, M.: The acid effect in the formation of 2-methyltetrols from the photooxidation of isoprene in the presence of NOx, Atmos. Res., 98, 2–4, 183-189, 2010.

Tawfik, A. B., and Steiner, A. L.: A proposed physical mechanism for ozone-meteorology correlations using land–atmosphere coupling regimes, Atmos. Environ., 72, 50-59, 2013.

Teng, A., Crounse, J., Lee, L., St Clair, J., Cohen, R., and Wennberg, P.: Hydroxy nitrate production in the OH-initiated oxidation of alkenes, Atmos. Chem. Phys., 15, 8, 4297-4316, 2015.

Tong, D. Q., Lamsal, L., Pan, L., Ding, C., Kim, H., Lee, P., Chai, T., Pickering, K. E., and Stajner, I.: Long-term NOx trends over large cities in the United States during the great recession: Comparison of satellite retrievals, ground observations, and emission inventories, Atmos. Environ., 107, 70-84, 2015.

Toon, O. B., Maring, H., Dibb, J., Ferrare, R., Jacob, D. J., Jensen, E. J., Luo, Z. J., Mace, G. G., Pan, L. L., Pfister, L., Rosenlof, K. H., Redemann, J., Reid, J. S., Singh, H. B., Thompson, A. M., Yokelson, R., Minnis, P., Chen, G., Jucks, K. W., and Pszenny, A.: Planning, implementation and scientific goals of the Studies of Emissions and Atmospheric Composition, Clouds and Climate Coupling by Regional Surveys (SEAC4RS) field mission, J. Geophys. Res., 121, 4967-5009, 2016.

Tost, H., Jöckel, P., Kerkweg, A., Pozzer, A., Sander, R., and Lelieveld, J.: Global cloud and precipitation chemistry and wet deposition: tropospheric model simulations with ECHAM5/MESSy1, Atmos. Chem. Phys., 7, 10, 2733-2757, 2007.

Trainer, M., Parrish, D. D., Goldan, P. D., Roberts, J., and Fehsenfeld, F. C.: Review of observation-based analysis of the regional factors influencing ozone concentrations, Atmos. Environ., 34, 12–14, 2045-2061, 2000.

Travis, K. R., Jacob, D. J., Fisher, J. A., Kim, P. S., Marais, E. A., Zhu, L., Yu, K., Miller, C. C., Yantosca, R. M., Sulprizio, M. P., Thompson, A. M., Wennberg, P. O., Crounse, J. D., St. Clair, J. M., Cohen, R. C., Laughner, J. L., Dibb, J. E., Hall, S. R., Ullmann, K., Wolfe, G. M., Pollack, I. B., Peischl, J., Neuman, J. A., and Zhou, X.: Why do models overestimate surface ozone in the Southeast United States?, Atmos. Chem. Phys., 16, 21, 13561-13577, 2016.

Val Martin, M., Heald, C. L., and Arnold, S. R.: Coupling dry deposition to vegetation phenology in the Community Earth System Model: Implications for the simulation of surface O 3, Geophys. Res. Lett., 41, 8, 2988–2996, 2014.

Warneke, C., Trainer, M., de Gouw, J. A., Parrish, D. D., Fahey, D. W., Ravishankara, A. R., Middlebrook, A. M., Brock, C. A., Roberts, J. M., Brown, S. S., Neuman, J. A., Lerner, B. M., Lack, D., Law, D., Hübler, G., Pollack, I., Sjostedt, S., Ryerson, T. B., Gilman, J. B., Liao, J., Holloway, J., Peischl, J., Nowak, J. B., Aikin, K. C., Min, K. E., Washenfelder, R. A., Graus, M. G., Richardson, M., Markovic, M. Z., Wagner, N. L., Welti, A., Veres, P. R., Edwards, P., Schwarz, J. P., Gordon, T., Dube, W. P., McKeen, S. A., Brioude, J., Ahmadov, R., Bougiatioti, A., Lin, J. J., Nenes, A., Wolfe, G. M., Hanisco, T. F., Lee, B. H., Lopez-Hilfiker, F. D., Thornton, J. A., Keutsch, F. N., Kaiser, J., Mao, J., and Hatch, C. D.: Instrumentation and measurement strategy for the NOAA

SENEX aircraft campaign as part of the Southeast Atmosphere Study 2013, Atmos. Meas. Tech., 9, 7, 3063-3093, 2016.

Wolfe, G., Hanisco, T., Arkinson, H., Bui, T., Crounse, J., Dean‐Day, J., Goldstein, A., Guenther, A., Hall, S., and Huey, G.: Quantifying sources and sinks of reactive gases in the lower atmosphere using airborne flux observations, Geophys. Res. Lett., 42, 19, 8231-8240, 2015.

Wu, S., Mickley, L. J., Jacob, D. J., Rind, D., and Streets, D. G.: Effects of 2000–2050 changes in climate and emissions on global tropospheric ozone and the policy-relevant background surface ozone in the United States, J. Geophys. Res., 113, D18312, 2008.

Xing, J., Mathur, R., Pleim, J., Hogrefe, C., Gan, C. M., Wong, D. C., Wei, C., Gilliam, R., and Pouliot, G.: Observations and modeling of air quality trends over 1990–2010 across the Northern Hemisphere: China, the United States and Europe, Atmos. Chem. Phys., 15, 5, 2723-2747, 2015.

Xiong, F., McAvey, K. M., Pratt, K. A., Groff, C. J., Hostetler, M. A., Lipton, M. A., Starn, T. K., Seeley, J. V., Bertman, S. B., Teng, A. P., Crounse, J. D., Nguyen, T. B., Wennberg, P. O., Misztal, P. K., Goldstein, A. H., Guenther, A. B., Koss, A. R., Olson, K. F., de Gouw, J. A., Baumann, K., Edgerton, E. S., Feiner, P. A., Zhang, L., Miller, D. O., Brune, W. H., and Shepson, P. B.: Observation of isoprene hydroxynitrates in the southeastern United States and implications for the fate of NOx, Atmos. Chem. Phys., 15, 19, 11257-11272, 2015.

Xiong, F., Borca, C. H., Slipchenko, L. V., and Shepson, P. B.: Photochemical degradation of isoprene-derived 4,1-nitrooxy enal, Atmos. Chem. Phys., 16, 9, 5595-5610, 2016.

Xu, L., Suresh, S., Guo, H., Weber, R. J., and Ng, N. L.: Aerosol characterization over the southeastern United States using high-resolution aerosol mass spectrometry: spatial and seasonal variation of aerosol composition and sources with a focus on organic nitrates, Atmos. Chem. Phys., 15, 13, 7307-7336, 2015.

Yahya, K., Wang, K., Campbell, P., Glotfelty, T., He, J., and Zhang, Y.: Decadal evaluation of regional climate, air quality, and their interactions over the continental US and their interactions using WRF/Chem version 3.6.1, Geosci. Model Dev., 9, 2, 671-695, 2016.

Yienger, J. J., and Levy, H. I.: Empirical model of soil-biogenic NOx emissions, J. Geophys. Res., 1001, D6, 11447-11464, 1995.

Yu, K., Jacob, D. J., Fisher, J. A., Kim, P. S., Marais, E. A., Miller, C. C., Travis, K. R., Zhu, L., Yantosca, R. M., Sulprizio, M. P., Cohen, R. C., Dibb, J. E., Fried, A., Mikoviny, T., Ryerson, T. B., Wennberg, P. O., and Wisthaler, A.: Sensitivity to grid resolution in the ability of a chemical transport model to simulate observed oxidant chemistry under high-isoprene conditions, Atmos. Chem. Phys., 16, 7, 4369-4378, 2016.

Atmos. Chem. Phys. Discuss., https://doi.org/10.5194/acp-2017-606
Manuscript under review for journal Atmos. Chem. Phys.
Discussion started: 13 July 2017

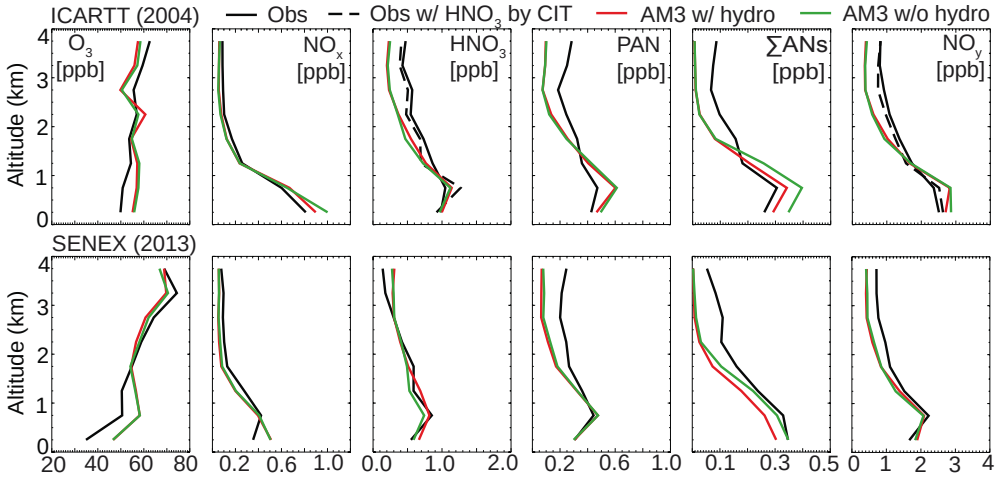

Figure 1. Mean vertical profiles of ozone and reactive nitrogen species from observations during ICARTT (top row) and SENEX (bottom row) over SEUS (25-40° N, 100-75° W) during daytime, and model estimates from AM3 with hydrolysis of alkyl nitrates (red) and AM3 without hydrolysis of alkyl nitrates (green). The dashed and solid black lines in the HNO_3 of ICARTT represent measurements collected using mist chamber/IC by University of New Hampshire (UNH) and Chemical Ionization Mass Spectrometer by California Institute of Technology (CIT), respectively. NO_y from ICARTT is calculated as the sum of NO_x, HNO_3 (w/ UNH in the solid line and w/ CIT in the dashed line), PAN and total alkyl nitrates (∑ANs). ∑ANs in the bottom row are from SEAC^{4}RS.

Atmos. Chem. Phys. Discuss., https://doi.org/10.5194/acp-2017-606
Manuscript under review for journal Atmos. Chem. Phys.
Discussion started: 13 July 2017

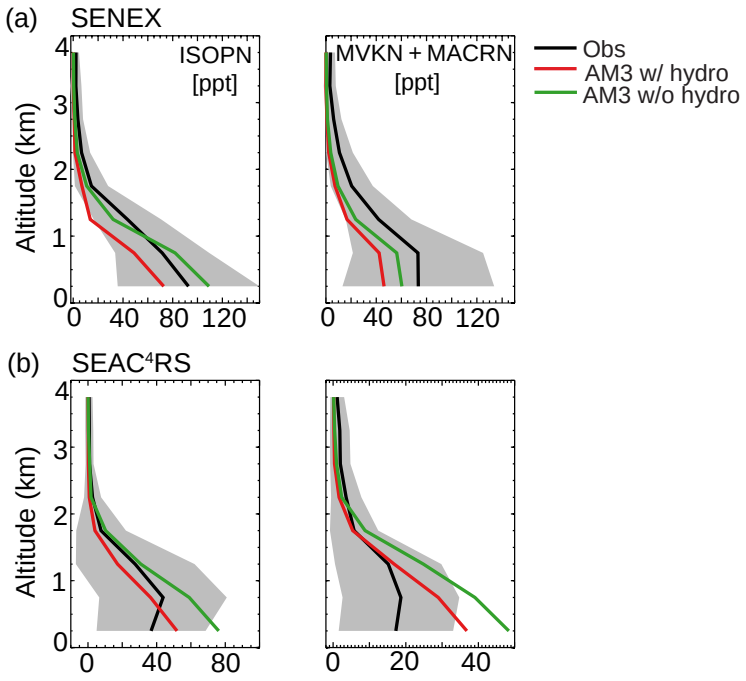

Figure 2. Mean vertical profiles of ISOPN and MVNK+MACRN during (a) SENEX and (b) SEAC^{4}RS over SEUS (25-40° N, 100-75° W). Black lines are the mean of observations. Red and green lines are the mean of modeled results with hydrolysis of ISOPNB and without hydrolysis of alkyl nitrates respectively. Grey shades are the one standard deviation (±σ) of averaged profiles of the measured tracers.

Atmos. Chem. Phys. Discuss., https://doi.org/10.5194/acp-2017-606
Manuscript under review for journal Atmos. Chem. Phys.
Discussion started: 13 July 2017

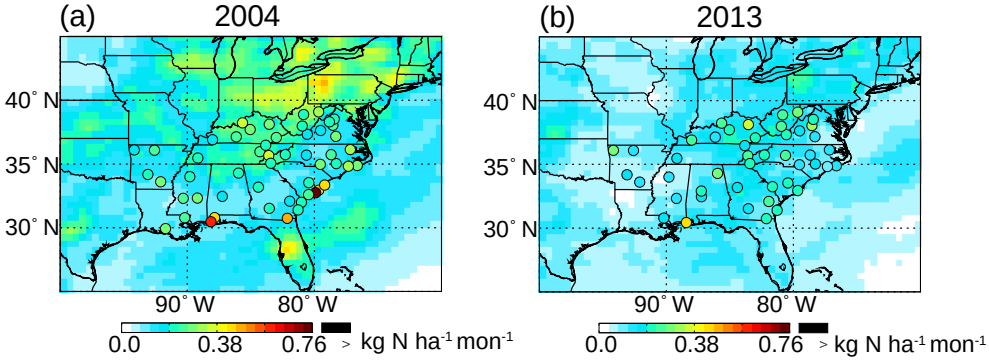

Figure 3. Nitrate wet deposition flux (kg N ha^{-1} mon^{-1}) from NADP (circles) and AM3 (background) during July-August of 2004 and 2013.

Atmos. Chem. Phys. Discuss., https://doi.org/10.5194/acp-2017-606
Manuscript under review for journal Atmos. Chem. Phys.
Discussion started: 13 July 2017

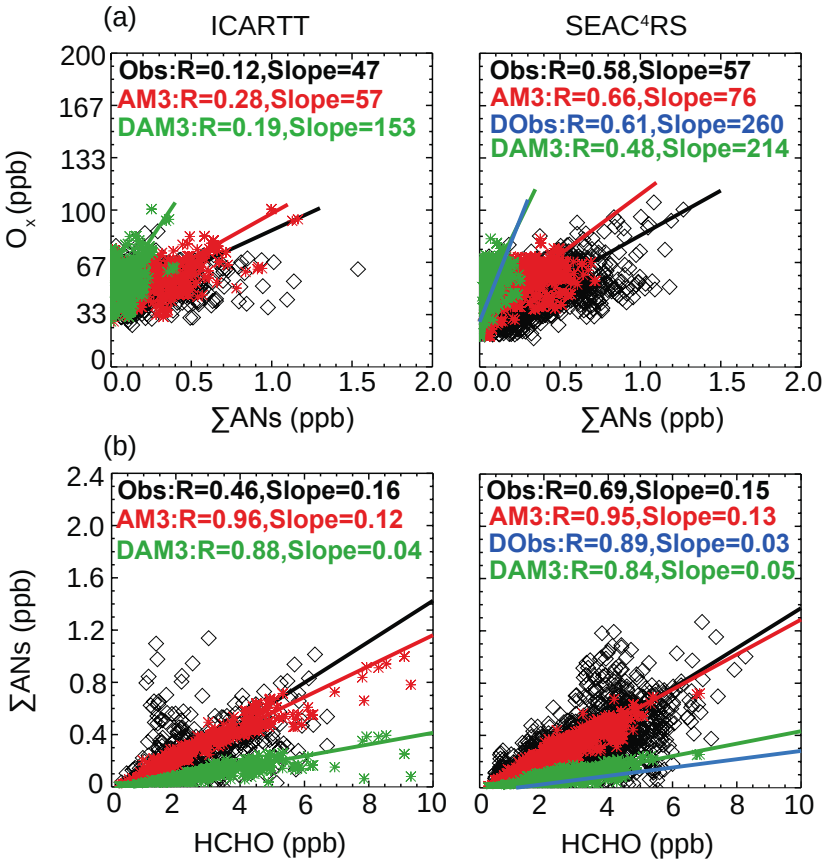

Figure 4. O_x versus ∑ANs correlation (top; (a)) and ∑ANs versus formaldehyde correlation (bottom; (b)) within the boundary layer (< 1.5 km) during ICARTT (left) and SEAC^{4}RS (right). Observations are in black diamonds; model estimates from AM3 with ISOPNB hydrolysis are in red symbols. Green symbols (DAM3) represent the correlation using modeled ISOPN + MVKN + MACRN. Blue symbols (DObs) represent the correlation using observed ISOPN + MVKN + MACRN from SEAC^{4}RS. Solid lines are the reduced major axis regression lines.

Atmos. Chem. Phys. Discuss., https://doi.org/10.5194/acp-2017-606
Manuscript under review for journal Atmos. Chem. Phys.
Discussion started: 13 July 2017

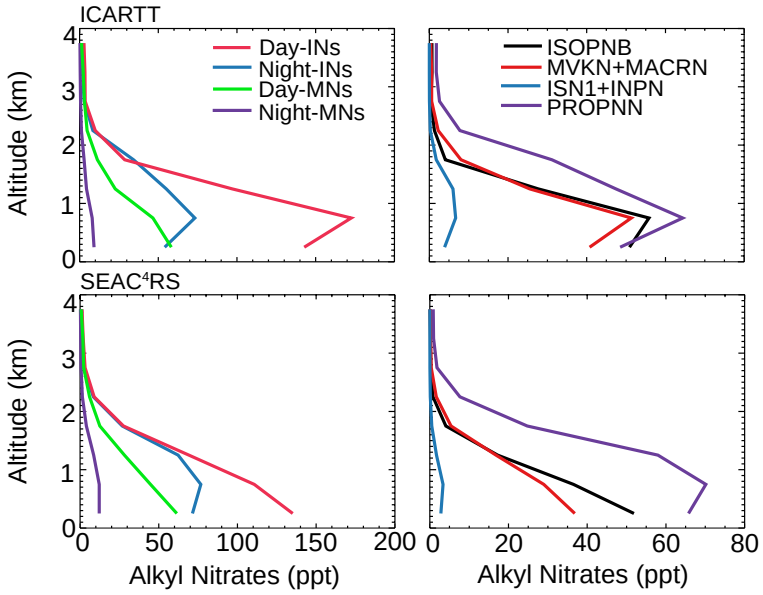

Figure 5. Mean vertical profiles of modeled alkyl nitrates from isoprene and monoterpene oxidation (left) and major isoprene nitrate species (right) during ICARTT (top row) and SEAC^{4}RS (bottom row) from AM3 with hydrolysis of ISOPNB.

Atmos. Chem. Phys. Discuss., https://doi.org/10.5194/acp-2017-606
Manuscript under review for journal Atmos. Chem. Phys.
Discussion started: 13 July 2017

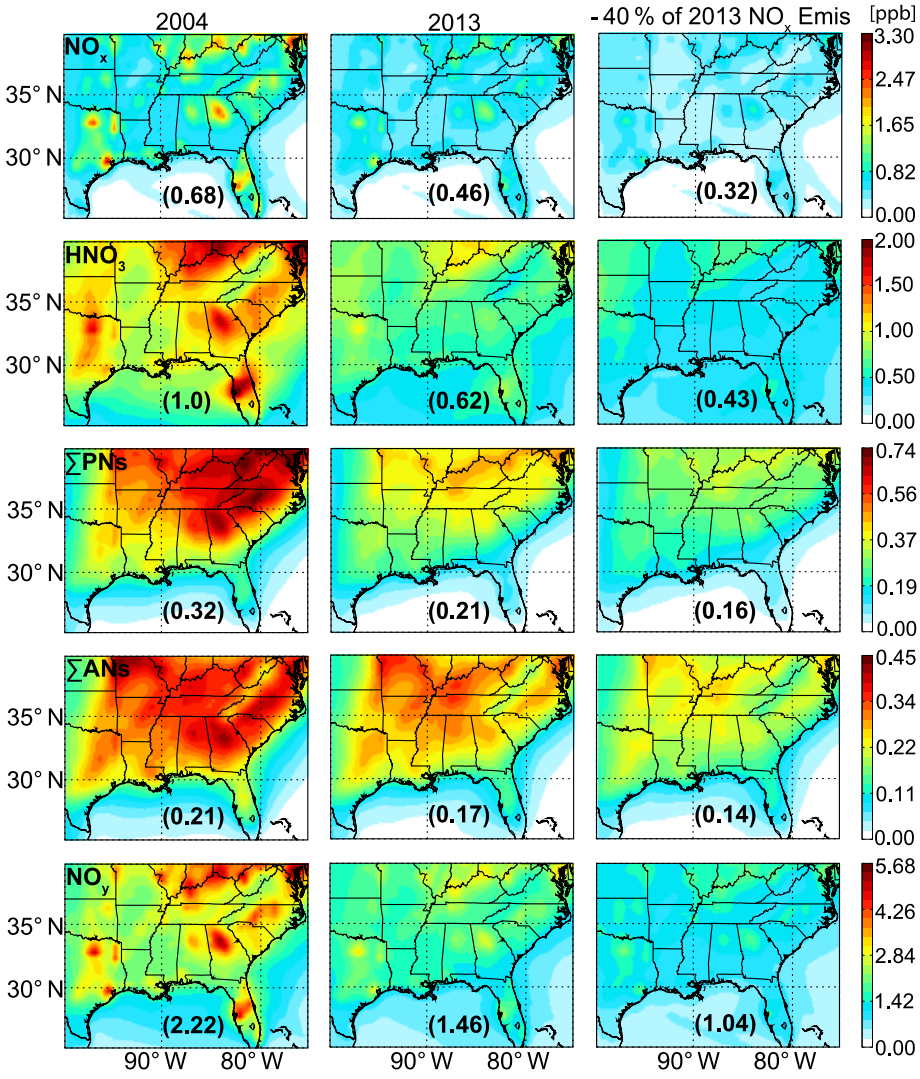

Figure 6. Modeled mean NO_x, HNO_3, total peroxy nitrates (∑PNs), total alkyl nitrates (∑ANs) and NO_y averaged over the boundary layer (< 1.5 km) of the Southeast U.S. during July-August of 2004 (left), 2013 (middle), and a scenario assuming 40 % reduction of 2013 anthropogenic NO_x emissions (right). Numbers in parentheses indicate mean concentrations over the plotted region. Note different color scales represent the concentration of each species.

Atmos. Chem. Phys. Discuss., https://doi.org/10.5194/acp-2017-606
Manuscript under review for journal Atmos. Chem. Phys.
Discussion started: 13 July 2017

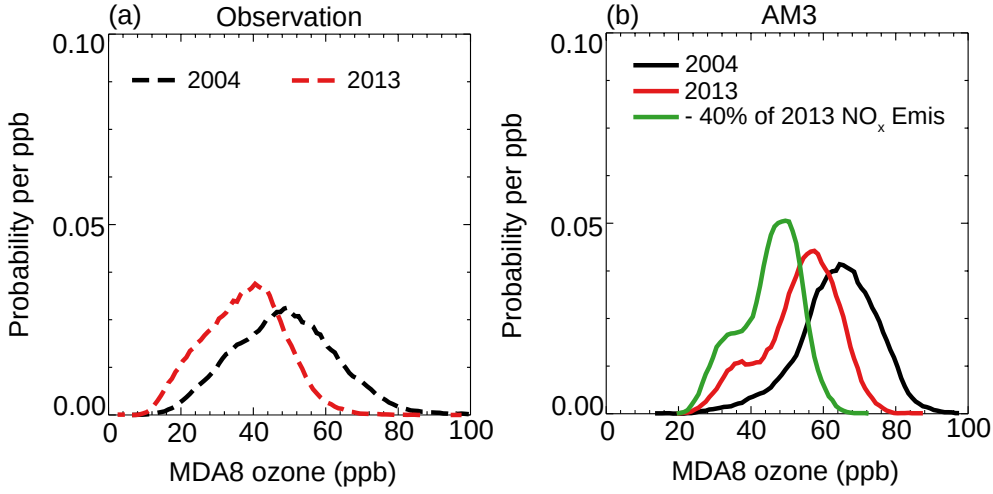

Figure 7. Observed (a) and simulated (b) probability density function of MDA8 ozone at AQS monitoring sites in Figure S3 during summer of 2004, 2013, and a scenario with 40 % reduction in the anthropogenic NO_x emissions of 2013.

Atmos. Chem. Phys. Discuss., https://doi.org/10.5194/acp-2017-606
Manuscript under review for journal Atmos. Chem. Phys.
Discussion started: 13 July 2017

Table 1. Monthly averaged NO_x emissions in July-August of 2004 and 2013 over North America (25-50° N, 130-70° W) in AM3.

Source Type	2004 (Tg N)	2013 (Tg N)
Anthropogenic	0.42	0.25
Biomass Burning	8.4×10^{-3}	8.4×10^{-3}
Soils	2.9×10^{-2}	2.9×10^{-2}
Aircraft	8.8×10^{-3}	8.0×10^{-3}
Lightning	0.02	0.02
Total	0.49	0.32

Atmos. Chem. Phys. Discuss., https://doi.org/10.5194/acp-2017-606
Manuscript under review for journal Atmos. Chem. Phys.
Discussion started: 13 July 2017

Table 2. Monthly NO_y budget in the boundary layer (< 1.5 km) of the Southeast United States for July-August of 2004, 2013 and a scenario with 40 % reduction of anthropogenic NO_x emissions of 2013[a].

	2004					2013					- 40 % of 2013 Anthropogenic NO_x Emis				
Species	Emission	Chem (P-L)	Dry Dep	Wet Dep	Net Export	Emission	Chem (P-L)	Dry Dep	Wet Dep	Net Export	Emission	Chem (P-L)	Dry Dep	Wet Dep	Net Export
NO_x	208.7	-172.4	21.8	–	14.5	132.6	-105	14.2	–	13.4	88.3	-69.6	9.2	–	9.5
∑PNs[b]		15.2	5.7	–	9.5		10.3	3.9	–	6.4		7.7	3.0	–	4.7
∑ANs		24.3	14.3	6.2	3.8		19.4	11.4	4.7	3.3		15.4	9.1	3.9	2.4
day[c]		13.8	8.7	3.6	1.5		12.0	7.5	3.0	1.6		10.2	6.3	2.6	1.3
night[d]		10.5	5.6	2.6	2.4		7.4	4.0	1.7	1.7		5.3	2.8	1.3	1.1
HNO_3		131.7	77.8	57.6	-3.7		74.2	45.6	35.1	-6.5		45.8	29.2	25.6	-9.0
NO_y					24.1					16.6					7.6

[a]We define the boundary of Southeast US is 25-40° N, 100-75° W. All budget terms are in Gg N.
[b]∑PNs include PAN, peroxymethacryloyl nitrate (MPAN), and a C5 hydroxy peroxyacyl nitrate (C5PAN1) produced by oxidation of ISN1.
[c]Alkyl nitrates produced from oxidation of isoprene and monoterpenes by OH.
[d]Alkyl nitrates produced from oxidation of isoprene and monoterpenes by NO_3.